Urban Forestry & Urban Greening 89 (2023) 128111

Contents lists available at ScienceDirect

Urban Forestry & Urban Greening

journal homepage: www.elsevier.com/locate/ufug

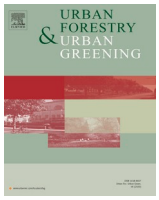

Original article

Urban green spaces and variation in cooling in the humid tropics: The case of Paramaribo

L. Best [a,*], N. Schwarz [b,1], D. Obergh [c], A.J. Teuling [d], R. Van Kanten [c], L. Willemen [e]

[a] Laboratory of Geo-Information Sciences and Remote Sensing group, Wageningen University and Research, P.O. Box 47, 6700 AA Wageningen, the Netherlands
[b] Faculty of Geoinformation Science and Earth Observation (ITC), Department of Urban Planning, Twente University, P.O. Box 217, 7500 AE Enschede, the Netherlands
[c] Tropenbos Suriname, Prof. dr. J. Ruinardlaan, CELOS Building, University Campus. P.O. Box 4194, Paramaribo, Suriname
[d] Hydrology and Quantitative Management group, Wageningen University and Research, P.O. Box 47, 6700 AA Wageningen, the Netherlands
[e] Faculty of Geoinformation Science and Earth Observation (ITC), Department of Natural Resources, Twente University, P.O. Box 217, 7500 AE Enschede, the Netherlands

ARTICLE INFO

Handling Editor:

Keywords:
Urban climate
Nature-based solution
Urban vegetation
Citizen science
Urban planning

ABSTRACT

The urban climate affects more than half the world's population, and urban green spaces are considered a nature-based solution to alleviate the urban heat island effect and adapt cities to climate change. Knowledge on urban green spaces cooling draws mostly on data from temperate climates, and similar research in humid tropical climates often focuses on the dry season. This study presents year-round temperature and humidity data for sixteen stationary sensors in Paramaribo, the capital of Suriname, and remotely sensed land surface temperatures for these locations. Analysis was done of diurnal and seasonal dynamics, the extent of urban green space cooling and the relation between locational characteristics and the micro-climate. Results show cooling up to 2.5 °C with distinct seasonal patterns, and that locations exhibiting stronger cooling during the day have smaller temperature ranges of about 4 °C at night compared to ranges of 5–7 °C at other locations. Locations with more trees and complex vegetation structure have temperatures that are 1–5 °C lower than other locations, but this cooling decreases when the ratio with impervious surfaces increases. Land surface temperature differences between more vegetated and built-up areas reach up to 2.5 °C. High correlations found among micro-climate indicators imply easier comparison between studies when using any of these indicators, even if not the same ones. The longer term data collected in our study enables investigating urban green space cooling taking into account seasonality typical to the humid-tropics and finds that this cooling can help cities in the Caribbean region adapt to temperature extremes, despite high humidity. Our study further provides an example for overcoming data scarcity and contributes to developing strategies for mitigating increasing heat-related health risks in the humid tropics.

1. Introduction

The warm urban climate in tropical cities affects millions of people. In 2018, about 1.5 billion people were living in urban areas in the tropics, and about 60 % of global urban growth until 2050 is estimated to take place in developing nations in the tropics (State of the Tropics, 2014, 2020). The negative effects of climate change, exacerbated by the urban heat island effect, increases the risks of higher temperatures in cities (Bowler et al., 2010). Warmer temperatures in cities affect people's lives in many ways, such as through higher energy consumption, increased greenhouse gas emissions, risks to human health, and positive feedbacks with air pollution (Giridharan and Emmanuel, 2018). Therefore, investigating urban cooling especially in the urban tropics is a pressing need.

Urban green spaces (UGS) are suggested as a strategy for climate adaptation in urban areas through their cooling effects (Aram et al., 2019; Bowler et al., 2010; Priya and Senthil, 2021). However, cooling from UGS varies across climatic regions (Liu et al., 2021), and so far, most urban climate studies were conducted in temperate climates, despite urban climate in the tropics being relevant for many city dwellers. Existing literature focuses on regions that only require heating of residential housing or combine heating and cooling of houses, so strategies cannot be readily translated to regions where only cooling is required (Bowler et al., 2010; Giridharan and Emmanuel, 2018; Roth,

* Corresponding author.
E-mail address: lisa.best@wur.nl (L. Best).
[1] Shared first authorship

https://doi.org/10.1016/j.ufug.2023.128111
Received 12 June 2023; Received in revised form 15 September 2023; Accepted 5 October 2023
Available online 6 October 2023

2007). As a result, scientific knowledge on UGS' cooling and urban climate in the humid tropics needs to be expanded to determine the most effective mitigation strategies (Aram et al., 2019; Bowler et al., 2010; Dobbs et al., 2019).

Two distinct aspects determine UGS cooling: the characteristics of i) the UGS and ii) the surroundings. First, vegetation type (e.g. grass, shrubs or trees), and plant structure characteristics (e.g. canopy density and leaf area index) determine the cooling capacity of UGS through shading and evapotranspiration (Richards et al., 2020). In the humid tropics, differentiating vegetation structure into single- or multi-layer vegetation is important (Li et al., 2020; Richards et al., 2020). Such multi-layer vegetation is often found in informal and, therefore, unmanaged UGS - and informality of public spaces is common in the Global South (Keeler et al., 2019). Unmanaged UGS often have tall, multi-layer vegetation with dense canopies similar to rural tropical vegetation. This tropical lush vegetation is characterized by high moisture availability, high thermal admittance, and lower albedo, leading to higher temperatures than in other climates and, therefore, lower cooling (Roth, 2007). At the city level, this also implies a lower temperature difference between built-up and surrounding rural green areas, i.e. a lower urban heat island intensity for tropical cities than in temperate cities of similar sizes (Roth, 2007).

Second, similar to temperate climates, more built-up areas lead to more sensible heat and less latent heat in the tropics (Giridharan and Emmanuel, 2018). At the micro level of individual UGS and pedestrian experience, an oasis effect of low air temperatures due to vegetation can often be detected (Chafer et al., 2022). In the humid tropics, these cooling effects were found to have a large range for different types of green infrastructure, from less than 1 °C up to 15 °C air temperature difference (Priya and Senthil, 2021). Thus, urban climate studies commonly use indicators describing the built-up surroundings and configuration of UGS (e.g., ratio of built-up area) (Park et al., 2017). Wetness is also important to consider in the tropics when distinguishing cooling effects in the wet and dry season, as wet or saturated surfaces lead to higher thermal admittance and, thus, less cooling (Chow and Roth, 2006).

Despite the knowledge on UGS cooling in the humid tropics, important research gaps remain. (1) Studies on UGS cooling are biased towards dry-, clear-sky conditions (Roth, 2007) and mostly cover less than 30 days. This results in a lack of studies that cover a full year and explore seasonal variation in the humid tropics (Feyisa et al., 2014; Priya and Senthil, 2021). (2) While several studies investigate the cooling effects of UGS characteristics, based on the land surface temperature (Feyisa et al., 2014; Masoudi et al., 2019) or diurnal air temperature patterns (Richards et al., 2020; Wang et al., 2022), only few studies consider these factors collectively (Aram et al., 2019). (3) Many studies on tropical urban climates are centered on air temperatures (Giridharan and Emmanuel, 2018), with few considering the effects of relative humidity. (4) A multitude of studies on UGS cooling result in highly varied information on temperature, such as daily average, day-time average, temperature range, temperature differences during the warmest time of day (Bowler et al., 2010). Although each context and research aim require specific information, for example, maximum temperature and hottest days in studies on extreme heat related to human well-being (e.g., Du et al., 2022), the lack of a standard for measures and information on the urban climate raises the question what to measure at the least, making it challenging to compare studies.

In this study, we address these four research gaps by exploring the urban climate characteristics at micro level (1) over a complete seasonal cycle and assess the relationship with urban vegetation and locational elements. We consider (2) air temperature, land surface temperature and (3) relative humidity simultaneously. (4) We analyze several micro-climate variables in parallel to explore their comparability. The aim of our study is to explore how UGS and other factors influence diurnal and seasonal micro-climate cooling. First, we describe the seasonal and diurnal patterns of air temperature, humidity, and land surface temperature at various locations within the city. Second, we quantify the cooling effects of UGS at the various locations. And third, we assess the relationship between the location characteristics and micro-climate variables. This study was conducted in Paramaribo, Suriname, located in the humid tropics. A citizen science monitoring initiative allowed covering a whole year for 16 locations across the city and provided the opportunity to reflect on this novel data collection approach.

2. Data and methods

2.1. Study area and overview

Paramaribo is the capital of Suriname, situated on the North-eastern rim of South America at about 1–21 m above sea level. Paramaribo has 241,000 inhabitants and a population density of around 1300 inhabitants per km2 (General Bureau of Statistics, 2021). The tropical rainforest climate (Af) has one short (December-January) and one long wet season (mid April to mid August) and two dry seasons (February to mid April, mid August to November) (General Bureau of Statistics, 2018). The average annual precipitation in Paramaribo is about 2200 mm, with the highest amounts generally in the long wet season, and the least during the long dry season (mid August-mid November) (Meteorological Service Suriname, 2023).

Paramaribo is a sprawling city (Fung-Loy et al., 2019; Weidum, 2014) with UGS interspersed in mostly low-density housing (Fig. 1). This, in combination with the lack of structural public UGS policies, is the main driver for conversion of UGS into built-up areas for housing or infrastructure development. Consequently, UGS consists mainly of grass and mixed low vegetation, largely found on abandoned private housing lots or uncultivated farmland. Other UGS include forest fragments and trees along streets and public squares in the downtown historic center. Public gardens or parks (e.g., Fig. 1, photo 4), sports fields and playgrounds with little or no trees in neighborhoods (e.g., Fig. 1, photo 18) are few.

The study builds on air temperature and humidity data collected in a citizen science project (groenparamaribo.org). The study first describes the seasonal and diurnal patterns of air temperature and humidity data (Section 2.2) from July 2021 to June 2022 at 16 stationary measurement locations. Second, the study quantifies and compares the cooling effects of these locations (Section 2.2). Land surface temperature (LST) was also described for each location (Section 2.3). Lastly, the relation of the cooling effects with the location characteristics is assessed (Section 2.4). The site selection aimed at covering a range of types and structure of vegetation, green versus built-up area ratio, unmanaged and managed UGS (e.g., photos 4, 16 and photos 2, 8 respectively) as well as densely built-up areas (e.g., photos 1, 11, 21), spread across the city (appendix Table A1, Fig. 1). Within these site requirements, citizens selected the specific location to place the sensors. This selection was based on the perceived relevance of that specific location (including use, recent land use change) and feasibility. They set up the sensor they "adopted" together with project staff and were responsible for replacing the battery, collecting the data through a mobile phone application and sharing them with project staff, cleaning the radiation shield (Section 2.2) if necessary and reporting on changes in the surroundings. These location characteristics are described in a 10 m (e.g., Schwarz et al., 2012) and 300 m buffer zone surrounding the temperature sensors (hereon: buffer) (Bao et al., 2016; Hamada & Ohta, 2010; Yan et al., 2014). The 10 m buffer was to account for any effects of the immediate surrounding on the measurement (Maclean et al., 2021).

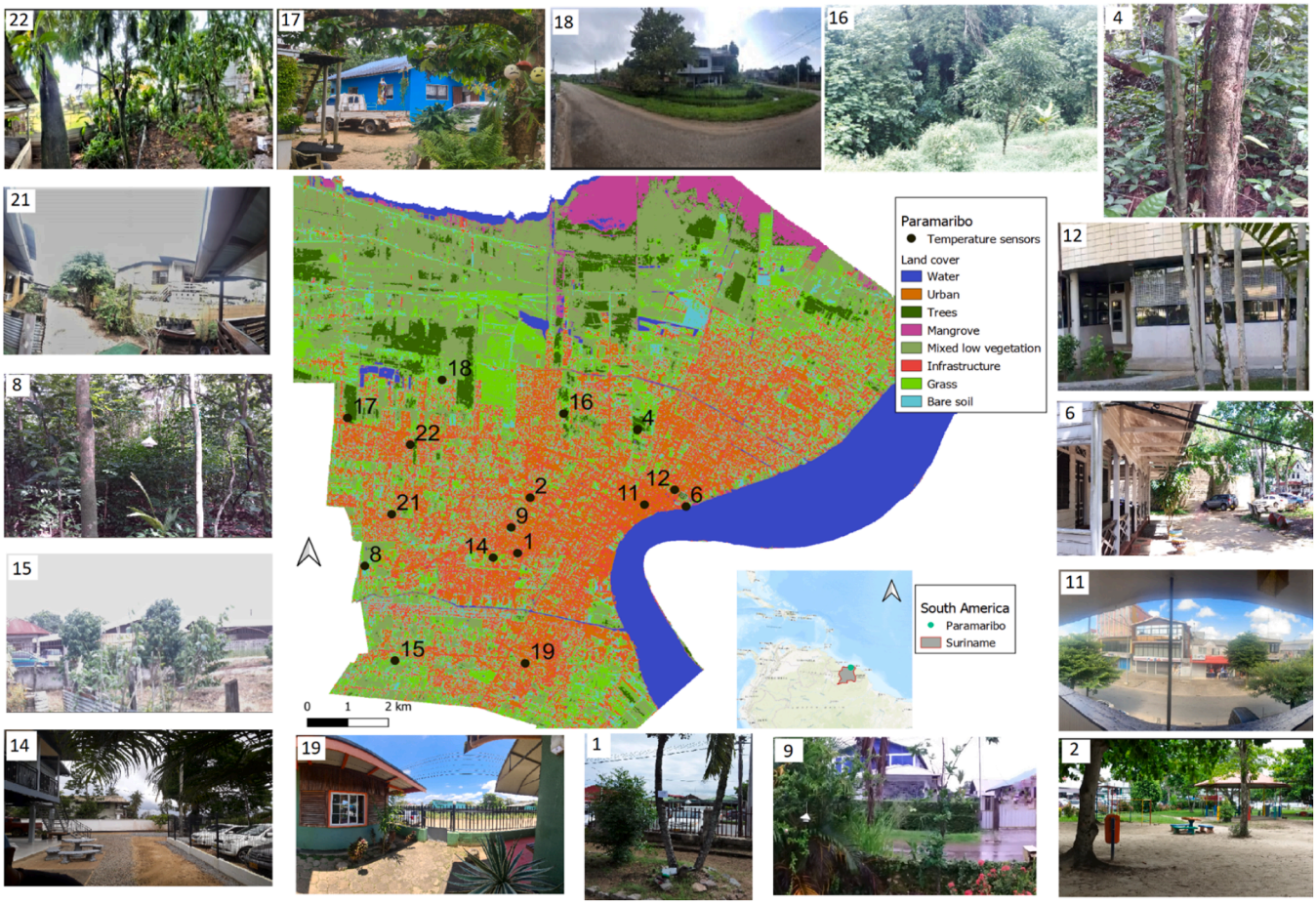

Fig. 1. Map of the study area and numbered measurement locations over land cover. (Taus et al., 2019).

2.2. Air temperature and humidity

Temperature and humidity were measured every hour with automatic wireless sensors (Kestrel D2) with a producer-stated accuracy of +/- 0.5 °C for temperature and +/- 2 % for humidity. Sensors were placed within a radiation shield following the guidelines in Hubbart (2011) to avoid direct sunlight heating up the sensor (World Meteorological Organization, 2021). Sensors were placed in accordance with WMO (2021) guidelines for urban areas and between 1.25 m and 3.00 m height, with larger heights to avoid sensors being within easy reach of passers-by. All locations were documented with GPS coordinates and a description of the surroundings (appendix Table A1).

When processing the data, erroneous time stamps of data logs were noted, especially briefly before a sensor battery ran out, so that temperature peaks were several hours off. Therefore, all data was visually checked and excluded if diurnal patterns were off or incomplete. Furthermore, we removed 4 days logged for one location that showed a sudden drop in humidity with almost no variation for unclear reasons. That led to 4592 logged days over sixteen locations, i.e., on average 287 days of measurements per location. For describing diurnal and seasonal temperature and humidity patterns, we used the hourly measurements and daily averages.

To quantify the cooling effects of UGS at the various locations, we first calculated the difference in temperature between each location and the average of all locations ($\Delta T = T_{Average} - T_{Sensor}$) using the seasonal means of each hour during a 24-hour period. We did not select one specific site as an "urban" or "rural" reference location (e.g., Hamada and Ohta, 2010) to avoid bias. Second, we compared the temperatures of all locations to each other at 6.00 hrs and 13.00 hrs, the coolest and warmest time of day, respectively, in the wet and dry season. And third, a similar comparison between locations is done for minimum night-time temperature, night-time temperature range and hot extremes. For determining the relationship of micro-climate variables and location characteristics (Section 2.4), we calculated aggregate micro-climate indicators based on their relevance for public health and thermal comfort:

- Mean annual and seasonal temperature and humidity as standard climatic indicators.
- Minimum local night-time (19:00 hrs to 6:00 hrs) temperature over the year and the season to indicate how well humans can rest at night (e.g., Obradovich et al., 2017).
- Range (i.e., the difference between maximum and minimum) of night-time temperatures to see how strongly temperatures decrease throughout the night.
- Hot extremes (Du et al., 2022; IPCC, 2021) quantified as maximum temperature and humidity on the ten hottest days identified across all locations (similar to Ebi et al., 2021).

2.3. Land surface temperature

The LST was calculated for the wet and dry season in the 300 m

buffers surrounding the sensor locations. LST was derived based on five-year seasonal composites of Landsat 8/9 OLI/TIRS images acquired via USGS Earth Explorer (appendix table A2) with a local overpass time around 11AM. Images were pre-processed in QGIS by masking for clouds using the CloudMasking plugin. LST was calculated based on the approach used in (Remijn et al., 2020), which includes atmospheric corrections, calculating brightness temperature, NDVI and surface emissivity. Wet season images had more clouds compared to dry season images, leading to lower-than-normal LST values around cloud edges after masking. Creating composite images allowed to fill in the masked pixels with the highest values in the same pixel in images from other years. This helped to reduce, if not eliminate, any cold edge pixels. For assessing the effect of UGS, the standardized LST (i.e., the difference between each pixel and the mean LST of all buffer areas divided by the standard deviation) of each seasonal composite image was used. To rule out any bias when creating the composite image, the LST standard deviation of the composite image was required to be within the same range as that of the individual images. This was checked using locations with no- (dry season) or the least cloud pixels (wet season).

2.4. Relation with location and green space characteristics

A variety of data was used to characterize the ground surface below the stationary sensors and their immediate and broader surroundings (Table 1) (e.g., Fu et al., 2022; Giridharan and Emmanuel, 2018; Li et al., 2020; Richards et al., 2020). The site data (Table 1) was gathered through field work, OpenStreetMap and the land cover shares through interpretation of a true color Maxar satellite image in the Bing repository in QGIS software, using randomly generated sample points. Due to the limited sample size (16), we used three categories for vegetation structure (in addition to no vegetation): grass and shrub; only trees and trees over shrubs, which in some cases includes forest fragments. Forests have a more dense and complex vegetation structure than, for example, a playground with shrubs beneath individual trees, but were aggregated with “trees over shrubs” to indicate multi-layer vegetation. To estimate the share of land cover in both buffers, a visual interpretation was conducted of trees, grass/shrub, impervious surface, bare soil and water, using 40 (50) randomly generated sampling points with a minimum distance of 2 m (10 m) for the 10 m (300 m) buffer.

Before analyzing the relationship between locational characteristics and micro-climate, we analyzed relationships among location characteristics and micro-climate indicators, respectively, to avoid collinearity and reduce the number of variables to consider. For numerical variables (e.g., share of land cover), we used Pearson correlations to exclude one variable out of a pair of variables with a significant and absolute correlation coefficient > 0.7. For the categorical location characteristics (e.g., surface cover below sensor), we investigated mosaic plots and boxplots, respectively, to identify close relations. Second, we investigated the relationships between location characteristics and micro-climate variables using Pearson correlations for numeric and Kruskal-Wallis tests for categorical location characteristics. For significant ($p < 0.05$) Kruskal-Wallis tests, we ran pairwise Wilcoxon rank sum tests to check for differences between groups. To adjust for multiple comparisons, we followed Vickerstaff et al., (2019) and used the Hommel adjustment for the correlations and the Wilcoxon tests. Due to the small sample size ($N = 16$), we refrained from more complex multivariate analyses.

3. Results

3.1. Seasonal and diurnal dynamics of temperature and humidity

Daily temperatures averaged over all locations were highest in September/October 2021 and lowest in February 2022 (Fig. 2, Table 2).

Table 1
Location and UGS characteristics used in the analysis.

Variable	Description	Variable format	Data source
Dominant surface cover below sensor and in 10 m buffer	Surface cover directly below the sensor or in 10 m buffer, respectively	Factor with levels = bare, bare with vegetation, vegetation, impervious, organic matter	Field work
Dominant vegetation structure in 10 m buffer	Classes describing multi- or single layer vegetation	Factor with levels = none, grass/shrub, only trees, trees over shrub/forest	Field work
Share of green (total) in 10 m and 300 m buffer in %	Share of trees, shrubs and grass in 10 m buffer	Metric, 0–1	Image interpretation
Share of tree (canopy) coverage in 10 m and 300 m buffer in %	Share of trees in 10 m buffer	Metric, 0–1	Image interpretation
Share of impervious in 10 m and 300 m buffer in %	Share of impervious surfaces in 10 m buffer	Metric, 0–1	Image interpretation
Distance to commercial center	Euclidean distance to densest point of commercial buildings	Metric, km	OSM: Commercial buildings selected from Points of interest shapefile, a heatmap identified the center of commercial buildings
Distance to river	Euclidean distance to Suriname river	Metric, km	OSM
Elevation	Elevation above sea level	Metric, m	Fieldwork

Average humidity values (Table 2) were high and varied between 83.7 % (October 2021) and 88.7 % (December 2021). The seasonal variation is clearly visible, with the wet season period from the end of July to the first half of August showing slightly higher temperatures than the December-January and May-June wet seasons. The first half of 2022 was exceptionally wet with several floods. Thus, the short dry season of February and March was wetter than a 10-year average (appendix Table A3). Consequently, we selected those months typically observed as the season peaks: October 2021 for the dry season and 15 May to 15 June 2022 for the wet season.

The spatial average LST from each location are clearly higher during the dry season (29–35.5 °C, standard deviations 0.4–2.3 °C) than the wet season (27–33 °C, standard deviations 0.5–1.8 °C) (Fig. 3). Thus, the seasonal LST are + /− 2–3 °C higher in the dry season and around 2 °C in the wet season than the air temperature values. Overall, the standard deviations of the air temperature (0.8–1.2 °C) are smaller than the LST standard deviations.

Diurnal dynamics show that air temperatures peak around noon, in the dry season somewhat earlier than in the wet season, while lowest temperatures are consistently recorded briefly before sunrise (Table 2, Fig. 4). The early morning hours show the lowest standard deviation of temperature across locations, i.e. temperatures are more similar across locations and over day of the year. The standard deviation of temperatures peaks in the afternoon (again, earlier in the dry season than in the wet season), meaning that temperatures in the afternoon are most variable across locations and the day of the year at that time. The standard

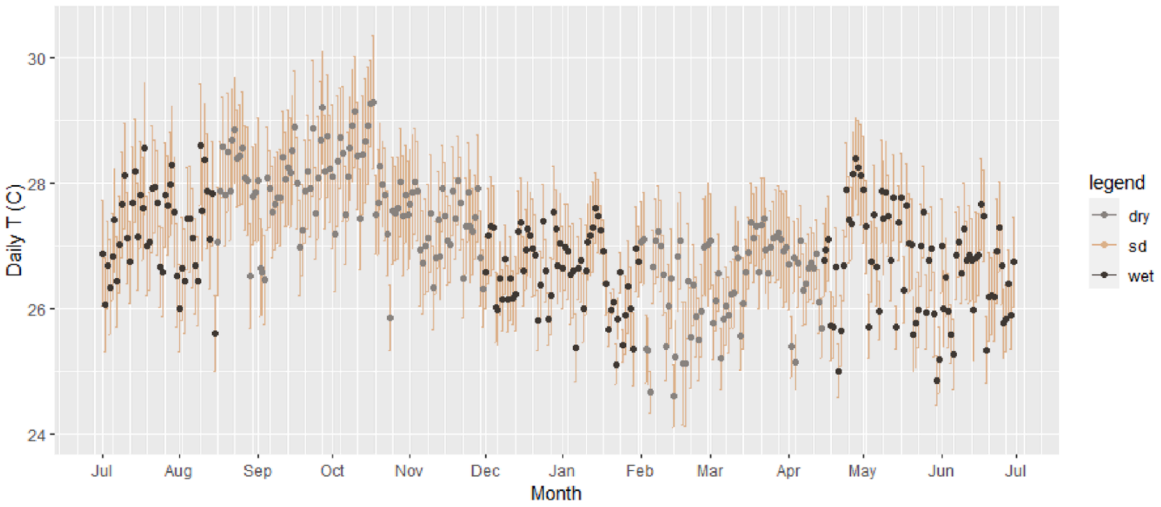

Fig. 2. Daily air temperature means (T) and standard deviations (sd) averaged across locations in the dry and wet season. Daily temperature means per location are provided in appendix Fig. A1a to A1k.

Table 2
Diurnal dynamics of temperature and humidity across locations.

	All year	Core dry season: Oct 21	Core wet season: 15 May - 15 June 22
Average temperature [°C]	27.0	28.0	26.5
Highest temperature mean [°C] during day	13:00 h 30.5 °C	12:00 h 32.1°C	13:00 h 29.4 °C
Lowest temperature mean [°C] during day	6:00 h 24.5 °C	6:00 h 25.1 °C	6:00 h 24.3 °C
Highest mean standard deviation of temperature [°C] during day	15:00 h 2.7 °C	13:00 h 3.2 °C	13:00 h 2.6 °C
Lowest mean standard deviation temperature [°C] during day	6:00 h 0.9 °C	7:00 h 0.8 °C	3:00 h 0.8 °C
Highest humidity mean [%] during day	7:00 h 94.9 %	6:00 h 95.0 %	7:00 h 95.5 %
Lowest humidity mean [%] during day	13:00 h 72.8 %	12:00 h 67.0 %	12:00 h 78.2 %
Highest mean standard deviation of humidity [%] during day	14:00 h 12.1 %	16:00 h 13.5 %	13:00 h 11.5 %
Lowest mean standard deviation humidity [%] during day	6:00 h 5.3 %	6:00 h 7.0 %	7:00 h 4.9%

deviation of temperature per hour is slightly higher in the dry season than in the wet season, probably due to more frequent precipitation limiting radiation and thus the surface control on temperatures. Humidity peaks consistently shortly after sunrise and is lowest at noon. In the dry season, the variation in humidity is highest in the late afternoon (16:00 h) but in the early afternoon for the wet season (13:00 h). Humidity is the least variable around sunrise.

3.2. The cooling effects

The extent of cooling of each location (Fig. 5) is up to 2.5 °C reduction compared to the average temperature, while heating reaches up to 3.5 °C, slightly less so in the wet season. Locations with more and multi-layer vegetation demonstrate higher relative humidity throughout the day (appendix Fig. A2) and larger temperature reductions (e.g., locations 4, 8, 2, 22) that are largest around noon. The cooling effect levels off between 18.00 and 19.00 h. Locations showing only small temperature differences to the average are typically residential areas, while locations with larger shares of impervious surface show increases. When comparing the temperatures at the warmest and coldest time of day in the dry season (Fig. 6a), the same locations again exhibit the lowest and highest temperatures (i.e., 4, 8, 2 and 22, and 11, 1 and 9, respectively). Locations with more open areas of grass or low vegetation (i.e., 15, 16 and 17) exhibit some of the lowest 6.00 h temperatures yet have warmer 13:00 h temperatures. Multi-layer vegetation is more effective at overall cooling throughout the day (e.g., 4, 2, 8), while locations with grass areas (i.e., single layer vegetation) appear more effective in releasing heat during the night (e.g., 15, 16, 17). The spread of the locations in Fig. 6 indicates stronger (large spread) or weaker (small spread) cooling. The wet season temperatures (Fig. 6b) are slightly lower than during the dry season and are spread less, showing clustering of temperatures and thus less cooling.

Night-time minimum temperatures across all locations are lower in the wet season compared to the dry season (Fig. 6c and d). The temperature range during the night, i.e. how strongly temperatures vary, is slightly larger in the dry season, and differences between locations are more notable in the dry season. Finally, the analysis of maximum temperature and humidity during the ten hottest days (Fig. 6e) reveals a considerable spread of temperatures (between 32 °C and 42 °C) between the locations with high overall humidity values (92–100 %), and higher tree coverage linked to higher humidity.

Average standardized LSTs over the period between 2018 and 2022 (Fig. 6f) show for most locations similar LSTs for the wet and dry seasons. Locations with negative LSTs values generally exhibit cooling and those with values above 0 generally exhibit warming compared to the average of all locations. In contrast to air temperature observations, locations 2 and 22 which had strong cooling effects, have slightly higher LST compared to the average. Overall, the greener locations show stronger cooling than locations with more impervious area and differences in LSTs reach around 2.5 °C in both seasons.

3.3. Relation between location characteristics and micro-climate variables

The correlations between the metric location characteristics show high - and expected - correlations ($|r| > 0.7$) (appendix Table A4). Thus, we removed the following location characteristics from further analysis: a) the distance to the river in favor of the distance to the CBD since the latter is more frequently used in similar analyses; b) the share of total green in the 10 m and the 300 m buffers in favor of the share of trees in

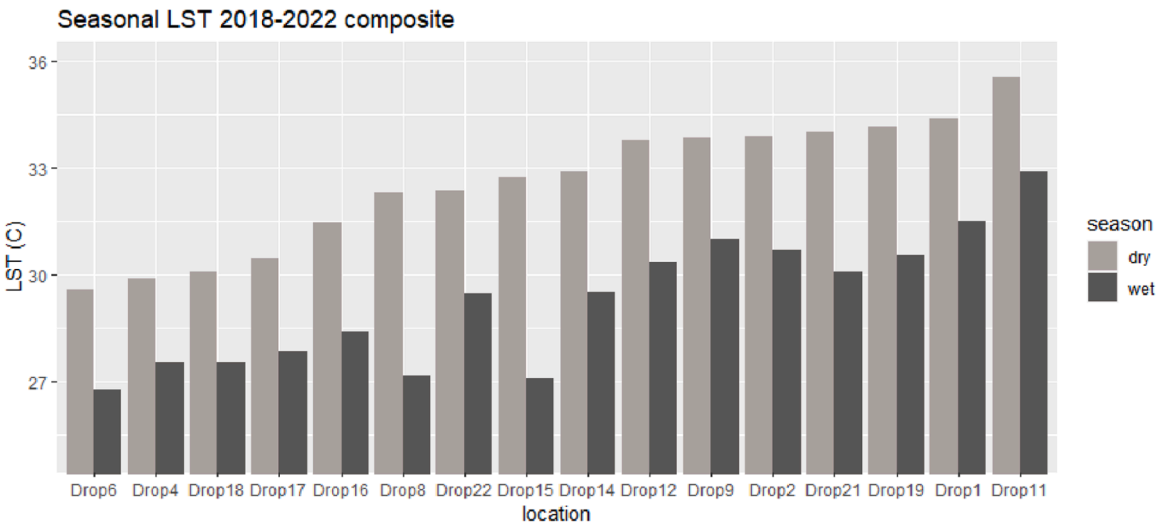

Fig. 3. Average land surface temperature (LST) per location in a 2018–2022 composite, differentiated between wet and dry season.

both buffers as the latter is more specific; and c) the share of impervious in the 10 m buffer to retain the share of trees in the 10 m buffer as we were more interested in the effects of vegetation cover. The mosaic plots among the location characteristics and boxplots between categorical and metric location characteristics (appendix Figs. A3a-c and A4a-c) show strong relationships between the dominant surface in the 10 m buffer and the share of land covers in the buffers. Thus, the dominant surface in the 10 m buffer was removed from further analysis.

We selected unique micro-climate variables based on correlations among the micro-climate variables to avoid high ($|r|>0.7$) correlations (appendix Table A5). Thus, we narrowed down the number of micro-climate variables to analyze further to the following: Mean annual temperature, minimum nighttime temperature for core dry and wet season, nighttime temperature ranges for core dry and wet season, mean humidity for wet and dry season, maximum humidity for the hot extremes, and average LST dry season. We removed the mean temperature in the wet and dry season, mean annual humidity and maximum temperature in hot extremes since they were highly correlated with mean annual temperature, and the latter is more frequently used in other studies. Furthermore, we removed the minimum nighttime annual temperature because it was highly correlated with the dry season minimum nighttime temperature, and we opted for keeping both seasons instead of the annual average and one season only. Similarly, we removed the annual nighttime temperature range due to its high correlation with dry season nighttime temperature range. We removed the LST wet season since the LST dry season had less cloud-coverage problems.

The correlation analysis revealed only two significant ($p < 0.05$) correlations between the location characteristics and the micro-climate variables (Table 3): The mean annual temperature is lower with higher shares of trees in the 10 m buffer, its high correlations with green (negative) and impervious land (positive) in the 300 m buffer are not significant. The average LST in the dry season is significantly correlated with the share of impervious land in the 300 m buffer. Other correlations are also high (e.g., mean humidity in the wet and dry season positively with the share of trees in the 300 m buffer) but not significant. To illustrate the effect of the share of trees in the 10 m buffer on mean annual temperature, we ran a linear regression with only these two variables (adjusted $R^2 = 0.59$, $p < 0.001$) and found a coefficient of -1.4, meaning that a plot with 100 % trees is 1.4 °C cooler than a plot without trees.

For the two categorical variables on the vegetation structure in the 10 m buffer around the sensor and the surface under the sensor (Fig. 7), only the Kruskal-Wallis test for vegetation structure and mean annual temperature was significant with $p < 0.05$ and significant pairwise differences (appendix Table A6). The pairwise comparison showed that forest/trees were significantly different from no vegetation, as well as only trees being different from forest/trees. Further Kruskal-Wallis tests were significant but no pairwise differences were found to be significant (appendix Table A6).

4. Discussion

4.1. Cooling effects of UGS in a tropical climate

Locations with more tree cover have stronger cooling effects than those with less tree cover, including during the hottest days (section 3.3). While this generally holds for the tree cover in both buffers, a few locations with higher shares of tree cover do not exhibit the strongest cooling, or even show slight heating (Fig. 5, appendix Table A1). Several reasons may be responsible: first, some locations have more tree cover in the 300 m buffer than in the 10 m buffer and show less cooling or even heating (e.g., locations 17 and 18). This is in line with the park distance theory (Feyisa et al., 2014; Jaganmohan et al., 2016), highlighting that cooling effects into the surroundings are stronger closer to the UGS. Second, in locations where this does not hold true (e.g., 6 and 16), additional factors that absorb or release heat may influence the cooling, such as impervious surfaces and traffic (Fu et al., 2022; Park et al., 2017), or the spatial configuration of UGS (Masoudi et al., 2019). The heating effect of impervious surfaces (Table 3) is in accordance with several other studies on LST (Feyisa et al., 2014; Masoudi et al., 2019), although Wang et al., (2022), using LST derived indicators, did not find significant correlations between anthropogenic characteristics and UGS cooling in the tropics.

Another significant relationship supported by previous studies in the humid tropics is that between the vertical vegetation structure and air temperature (Li et al., 2020; Park et al., 2017; Richards et al., 2020). In our study, forest fragments had the strongest cooling effect, and the limited number per vegetation structure in our study likely hindered more statistically significant results, also for the correlations with the share of trees in the buffers. The diurnal patterns show that the average temperature of all locations peaks around noon (Table 2), indicating that

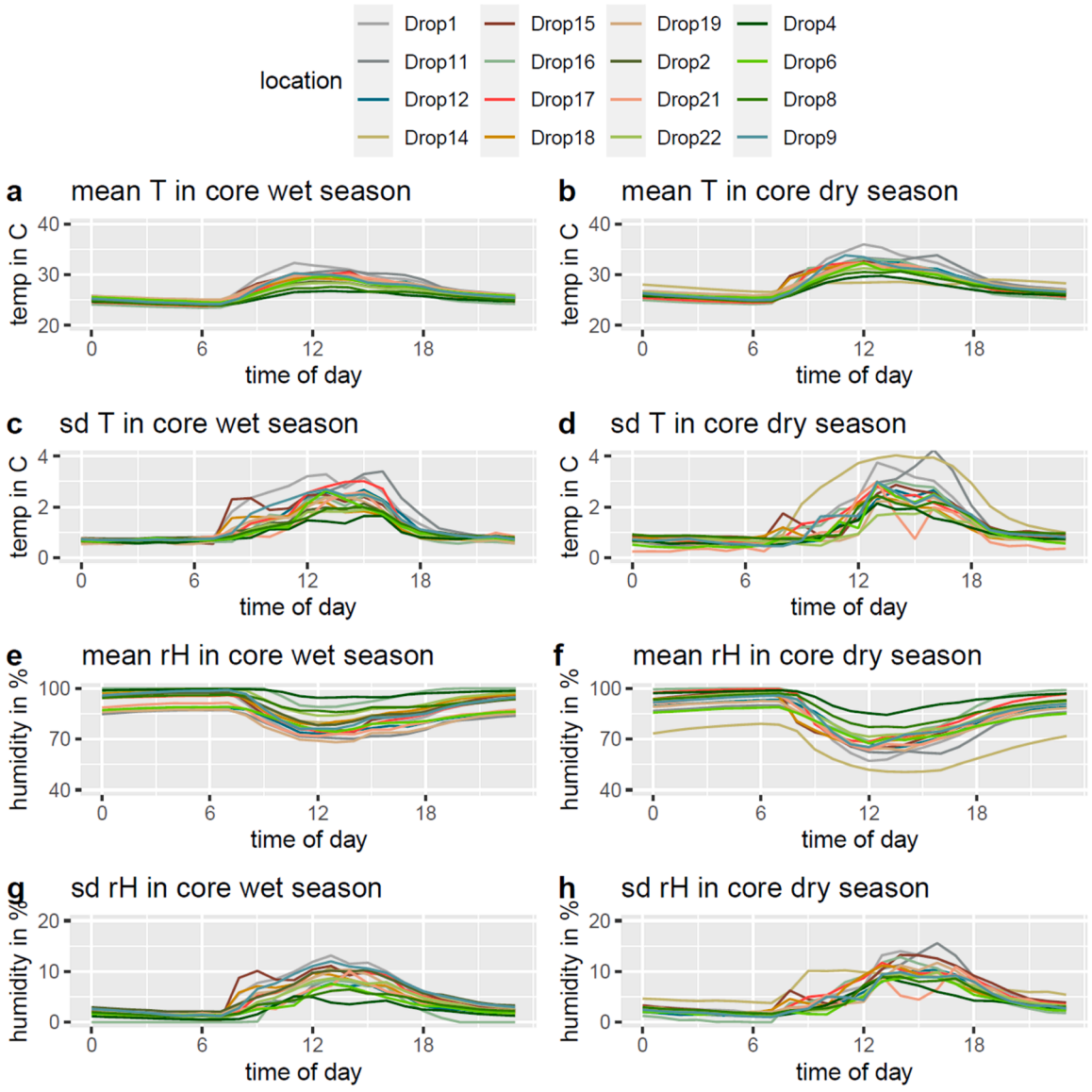

Fig. 4. Diurnal patterns of mean temperature (T), standard deviation (sd) of temperature, mean relative humidity (rH) and standard deviation of humidity per location throughout the day.

the more vegetated locations retain their lower temperatures during the morning hours until solar radiation becomes too high and heat from non-green surroundings invades (Park et al., 2017). Reduced cooling in UGS around noon may be due to reduced photosynthesis because plants close their stomata when solar radiation intensifies, or due to a possible threshold in cooling efficiency (Feyisa et al., 2014; Fu et al., 2022). The night-time cooling shows a similar pattern: Minimum night-time temperatures are lower for locations with lower shares of impervious surface. Notably, those with the lowest temperatures are located toward the outskirts of the city, where built-up areas become less dense and open spaces (e.g., for agriculture) are more common. More specifically, forest fragments were associated with lower minimum night-time temperatures, but single-layer vegetation, only consisting of trees, with smaller night-time temperature ranges (Fig. 7). Exploring these differences in vegetation structure will be important for future studies.

At the same time, the share of trees or the presence of forest fragments are related with higher humidity (as also found, for instance, by Li et al., (2020), as can be expected due to photosynthesis leading to more water vapor in the air. Higher humidity values are concerning for human well-being, as higher humidity is associated with less thermal comfort. The trade-off involving lower temperatures but higher humidity in forest fragments needs to be further studied to see whether the positive effect of lower temperatures outweighs the higher humidity. For a temperate urban climate, Ren et al., (2022) showed that relative humidity was not significantly correlated with human physiological stress parameters while temperatures were. Using outdoor thermal comfort-indices (for hot humid regions: Binarti et al., 2020) to further analyze is beyond the scope of this study but warranted in future research. Finally, we observed clear seasonal effects on cooling, with weaker cooling in the wet season compared to the dry season. This observation follows the

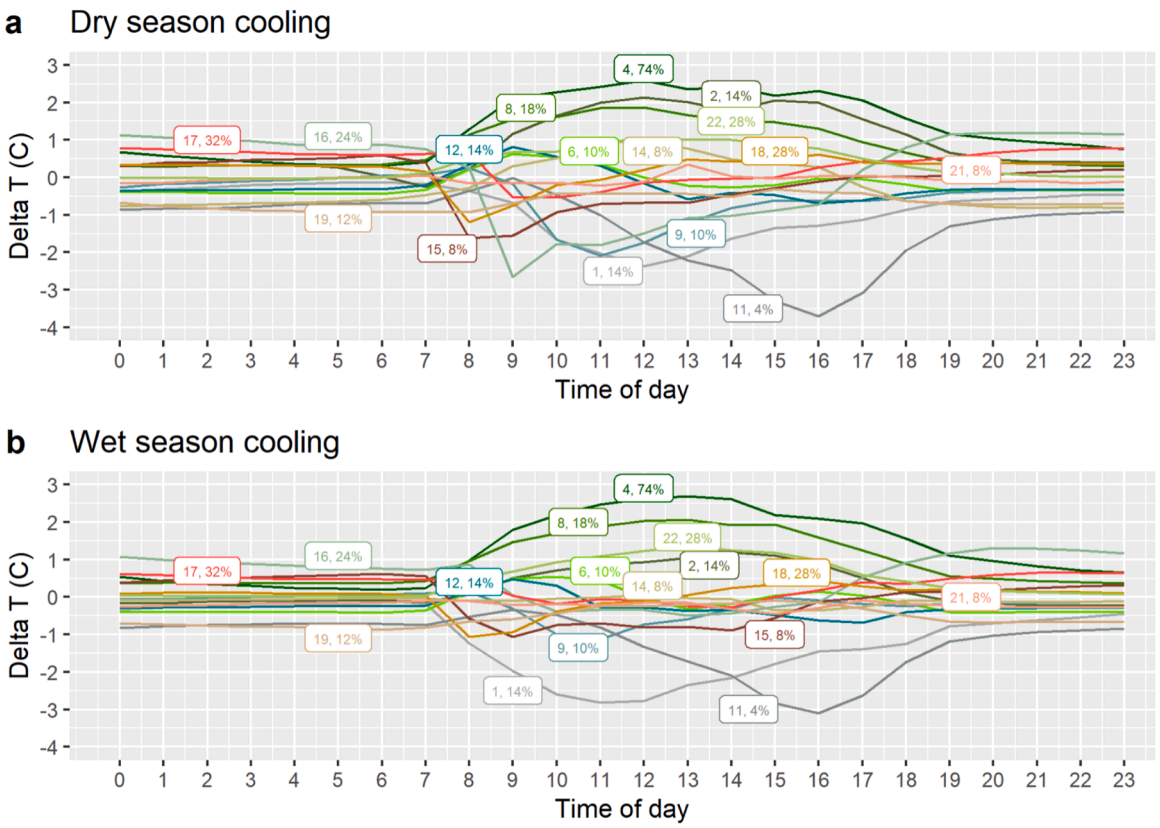

Fig. 5. Temperature (T) of measurement locations subtracted from the average of all locations, the numbers indicate the location IDs and tree cover% in the 300 m buffer. The lines below zero refer to negative temperature differences ($\Delta T = T_{Average} - T_{Sensor}$, Section 2.2), indicating heating, while the distance to zero indicates the extent. Dark green represents locations with more and complex vegetation, and gray larger shares of impervious surface.

expected impact of lower solar radiation, higher humidity as well as higher soil moisture in the wet season, which may lower the cooling effect of UGS in comparison to built-up areas (Chow and Roth, 2006). Unfortunately, few studies in similar climates cover at least a year to observe cooling effects during wet and dry seasons. To optimize cooling effects also for the wet season, more detailed insights into seasonal differences per vegetation type, and for UGS types on the spectrum of natural- to human-made environments, for example, are needed.

4.2. Urban climate indicators

The literature on the urban climate and cooling from UGS includes a variety of indicators to describe urban climate patterns and cooling effects, making comparability between studies a challenge. In our study, we started with sixteen indicators to describe the cooling effect from UGS on temperature and humidity patterns in parallel. Correlations among micro-climate indicators showed many similarities, such as between temperatures of the wet and dry season. Thus, studies each using one of these highly correlated indicators could be compared.

Nine micro-climate indicators were not highly correlated with others and, therefore, provide 'unique' angles to the micro-climate: mean annual temperature, mean humidity of the core wet and dry season, minimum night-time temperature for core dry and wet season, night-time temperature ranges for core dry and wet season, mean humidity during hot extremes and the average LST during the dry season. These indicators also have different implications for thermal comfort. To complement the minimum night-time temperatures (Obradovich et al., 2017), we introduced the range of night-time temperatures to see how strongly temperatures decrease throughout the night and found considerable ranges of up to 7.6 °C for the core dry season, indicating significant relief from heat stress at night. Three humidity-related indicators were found not to be significantly related with the air and land surface temperatures in our sample, indicating that future studies on urban green in the tropics should explore the role of relative humidity further.

Notably, the standardized LST in the dry season was only highly correlated with the LST in the wet season (Fig. 6f). Absolute correlations with all other micro-climate indicators were below 0.7, and all these indicators are based on air temperatures or humidity. These lower relationships point out the differences between air temperatures and LST. While air temperatures indicate temperatures in the canopy layer, i.e., the atmosphere from the ground up to building height (Arnfield, 2003), LST are measurements of the ground beneath. Urban air temperatures were found to be related to LST in temperate climates (e.g., Schwarz et al., 2012), the tropical Atlantic (Do Nascimento et al., 2022) and temperate vs tropical climate (Amorim et al., 2021). However, analyzing these relationships is challenging due to cloud coverage (Do Nascimento et al., 2022), an issue more prevalent in the tropics.

Overall, reporting several micro-climate indicators in parallel can improve comparability of studies as chances are higher that the same indicators are reported in several studies. Furthermore, conscious selection of indicators can provide insights into distinct aspects of the urban climate which may be more useful in certain contexts than others (e.g., health risks or energy consumption).

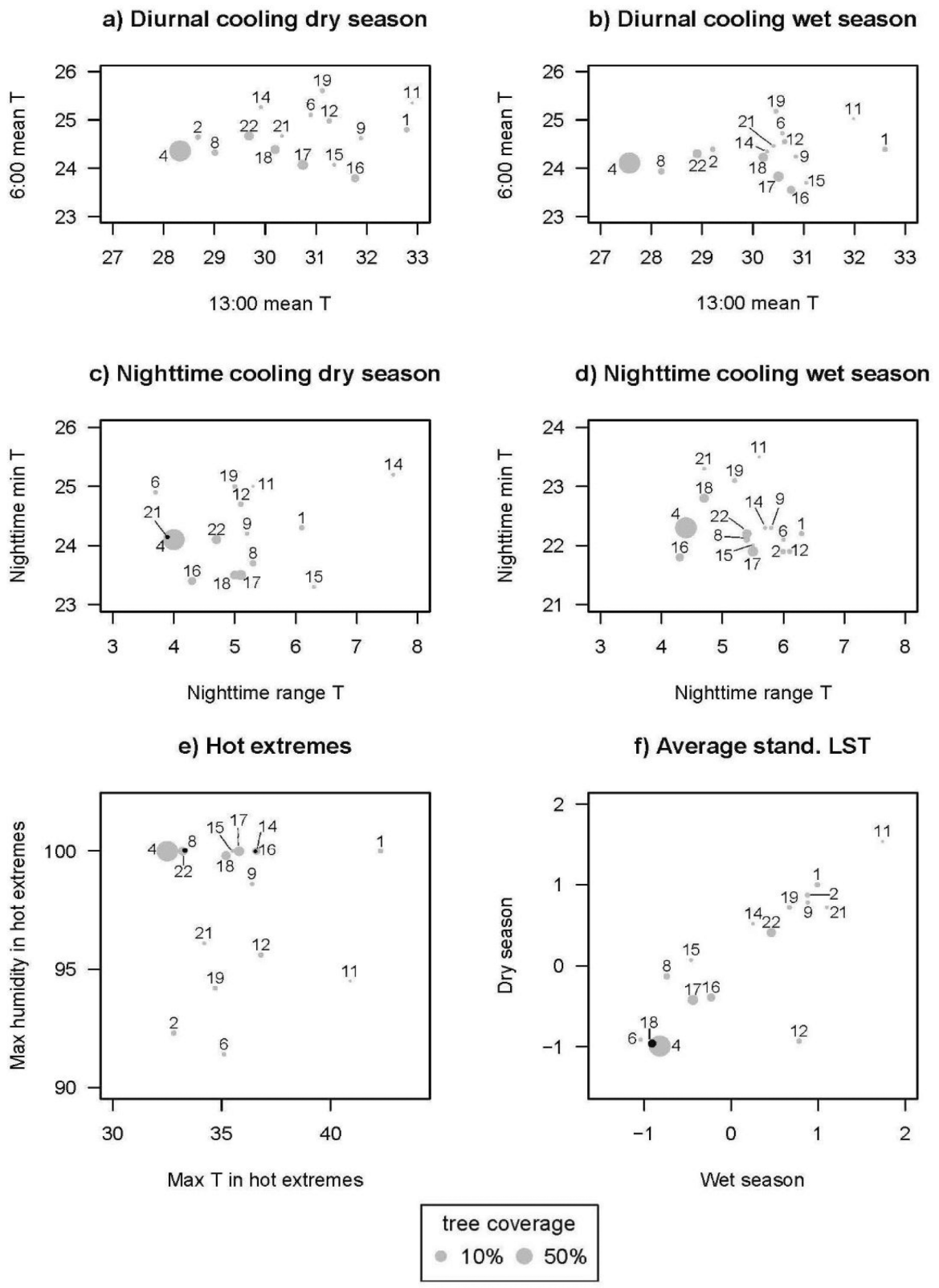

Fig. 6. Cooling effects across 16 locations in Paramaribo: temperature differences at the warmest vs. coolest time of day during the dry- (6a) and wet season (6b); night-time minimum and range of temperature in the dry- (6c) and wet season (6d), maximum temperature and humidity during the 10 hot extreme days (6e) and average standardized LSTs in the dry- and wet season (6 f).

Table 3
Pearson correlation coefficients and significance levels between location characteristics (rows) and micro-climate variables (columns), n = 16.

	Mean annual temperature	Mean humidity dry season	Mean humidity wet season	Min night-time temperature dry season	Min night-time temperature wet season	Night-time temperature ranges for dry season	Night-time temperature ranges for wet season	Maximum humidity hot extremes	Average land surface temperature dry season
Elevation	0.09	0.16	-0.06	0.02	0.26	-0.1	-0.14	-0.12	0.15
Distance to commercial center	-0.3	0.18	0.22	-0.61	-0.06	0.19	-0.26	0.53	-0.01
Share of trees (10 m)	-0.79 *	0.6	0.64	-0.3	-0.39	-0.32	-0.25	0.14	-0.27
Share of trees (300 m)	-0.7	0.65	0.63	-0.34	-0.22	-0.38	-0.54	0.4	-0.55
Share of impervious land (300 m)	0.74	-0.47	-0.6	0.58	0.55	0.2	0.37	-0.37	0.82 * *

* $p < 0.05$, * * $p < 0.01$

4.3. Mitigating urban heating

When quantifying the cooling effect based on location characteristics, the comparison between selected variables provides different angles to approach the mitigation of urban heating. For example, temperatures at the coldest time of day versus the warmest time of day can provide insights for UGS design interventions to maintain outdoor thermal comfort throughout the day, while differences between greener locations and the average temperature point to further research questions on which UGS types, vegetation structure or species could be most effective given the climate. As a mentioned above, the trade-off between higher humidity versus lower temperatures in dense forests should be further investigated in terms of impacts on human comfort. It is important to conduct more studies on heat mitigation in the tropics, as the relationship between land cover and temperatures varies between climate zones (as shown for LST by Naserikia et al., 2022) and little is known for the tropics.

The effectiveness of UGS as a cooling strategy depends not only on temperature reduction but also on the behavior of urban residents. In Suriname, urban residents usually adapt their daily activities to the climate according to the time of day. Outdoor activities take place in the morning or late afternoon, while people seek refuge in air-conditioned offices or homes during midday. Considering the behavior of residents is especially relevant from the perspective of inequality, to ensure that residents having to walk long distances, wait for public transport, or who do not have office jobs or air conditioning at home, are not disproportionately affected by temperature extremes and associated health risks in the humid tropics. What is more, using UGS for cooling may reduce energy consumption.

4.4. Reflection on citizen science approach

The advantage of the citizen science setup is that we were able to collect data over a longer period of time, in specific locations (thus not depending on fixed meteorological service weather stations) throughout wet and dry seasons. In contrast to studies in temperate climates, which often focus on summer seasons and clear-sky conditions for using the strongest UHI effects, cities in humid-tropical climates are hot year-round. Thus longer datasets are important, considering the seasonal variability and relative humidity, which is relevant for human thermal comfort and heat-stress, and allows better investigation into UGS as cooling strategies for urban planning and climate adaptation purposes in the humid tropics. Despite limitations in site selection for citizen data collection, the total number of sites expanded beyond those included in this study, enabling a larger geographical reach (Cooper et al., 2007; Sayer et al., 2015). This may have otherwise been challenging to achieve with conventional field data collection methods, due to geographic accessibility, logistical and financial barriers common in development contexts in the humid tropics (Klemann-Junior et al., 2017). Aside from helping overcome data scarcity and potentially covering under sampled regions, the citizen science participants also contribute with their knowledge of their local surroundings to contextual nuance for informed decision-making (Sayer et al., 2015). Although our study used automatic temperature loggers, citizens also filled in mobile surveys regarding any irregularities or changes in the surroundings which may affect the data measurements. In any case, it remains essential to explicitly consider and report on the careful selection of representative and comparable sites (Bowler et al., 2010). Finally, engaging with citizens in scientific projects can not only have influence on the science itself, but also have a variety of wider benefits for society (including the citizen scientists and their learning, raised awareness etc.), economy (e.g. economic benefits derived from data, new entrepreneurs), environment (if data-gathering is linked with conservation activities, for example), and governance (influence on policies) (Wehn et al., 2021).

4.5. Limitations of the study and future research

The limitations of our study relate to monitoring setup. First, the spatial extent of our study area is a sprawling city surrounded by mangroves, peri-urban areas and dense rainforest further inland. This makes it impossible to identify a rural reference location without built-up surroundings that is accessible for monitoring. Therefore, we did not observe the urban-rural heat island, but rather the heating within the urban area (Giridharan and Emmanuel, 2018). Second, trade-offs were made when selecting measurement sites between the representativeness (e.g., spread across the city) and citizen's preference, since our study is part of a citizen science monitoring project where citizens 'adopt' sensors measuring devices. Thus, the site selection considered accessibility, perceived importance by citizens, and practical convenience for the citizens, which led to slight shifts of measuring sites closer to participants' home or UGS they regularly visit. The exact location of the sensors was also adapted to lower the risks of theft or vandalism. Therefore,

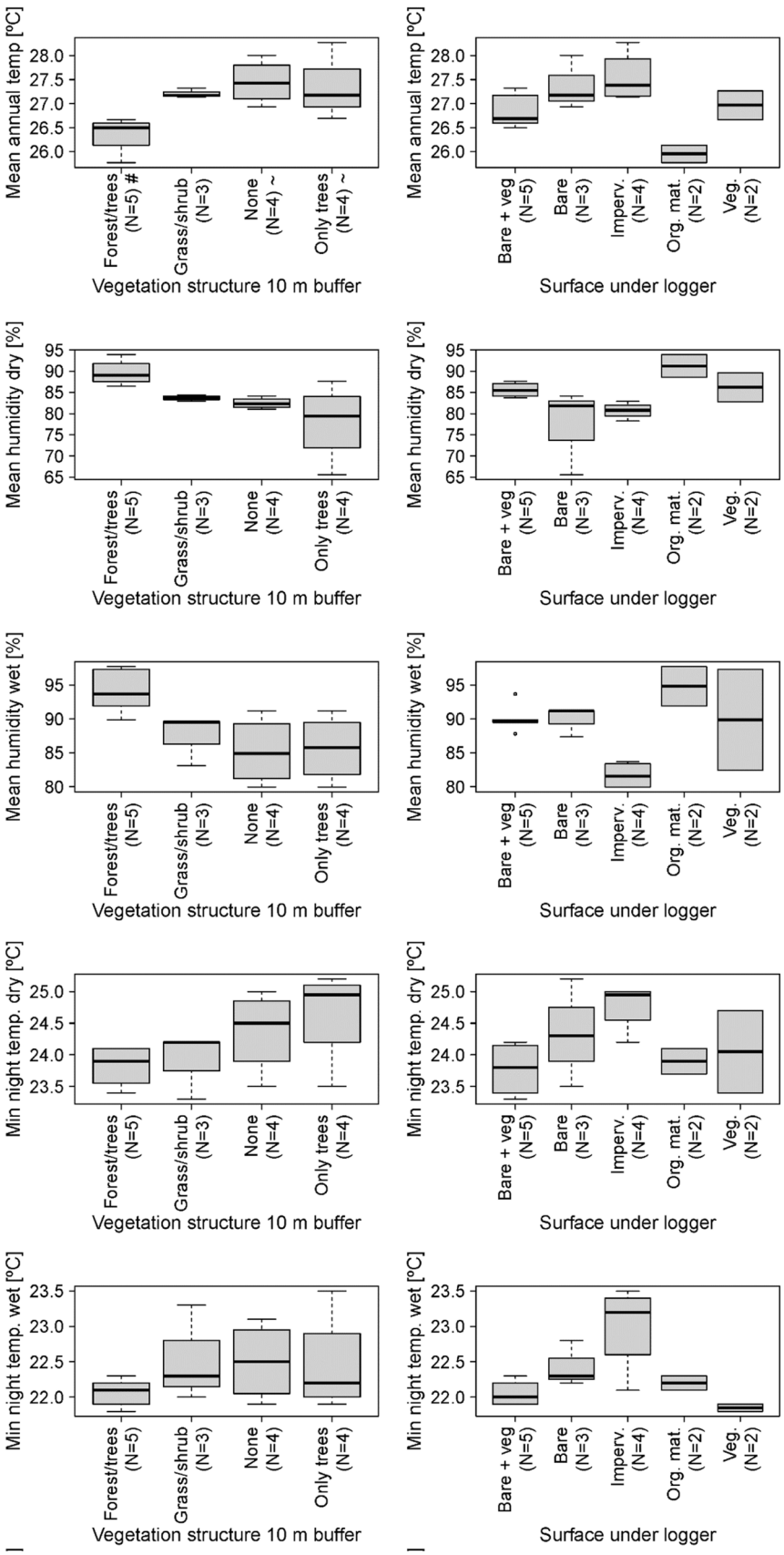

Fig. 7. Boxplots between vegetation structure in 10 m buffer and surface under the stationary sensor with micro-climate variables. ~and #: significant differences between groups in Kruskal-Wallis test.

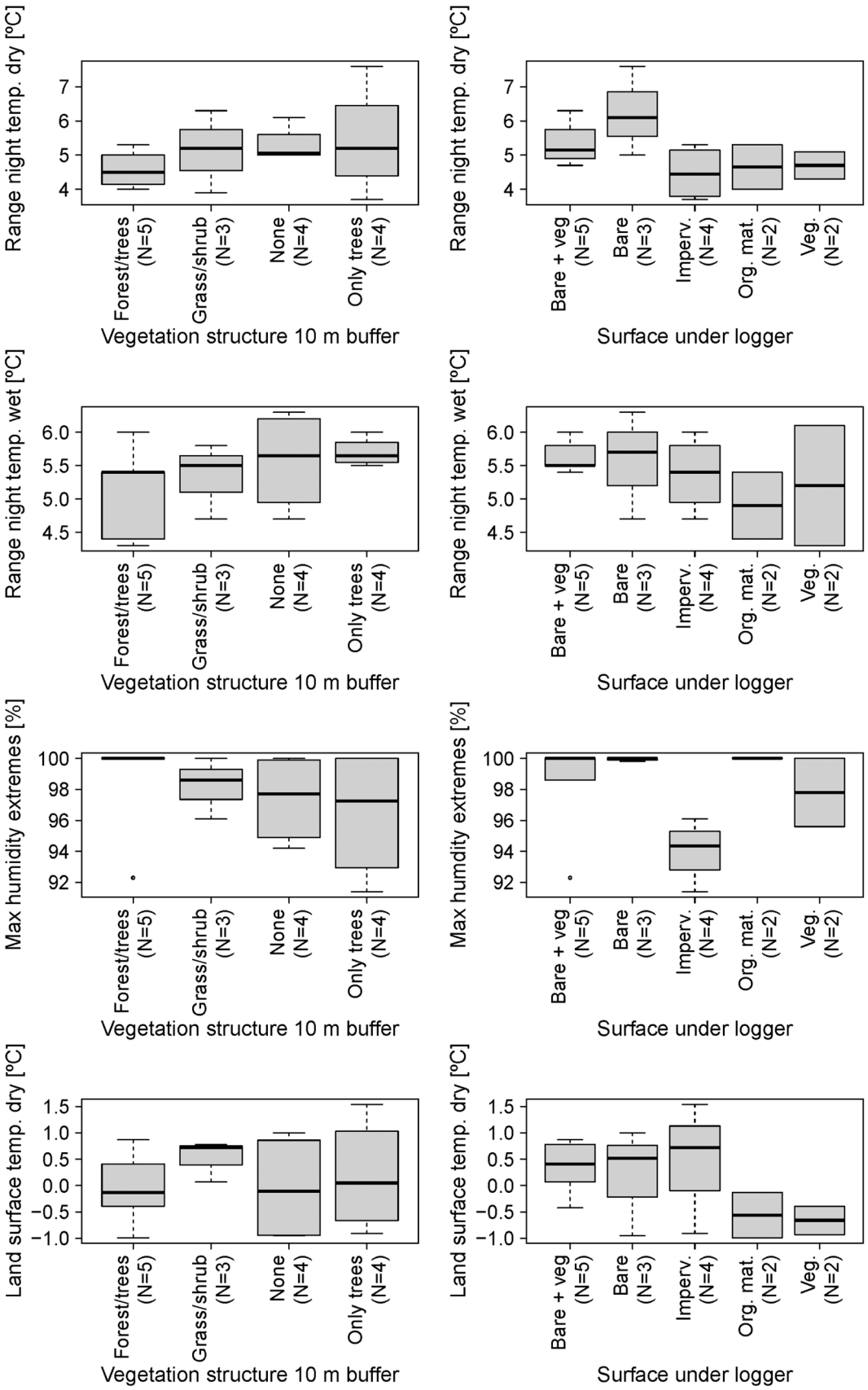

Fig. 7. (*continued*).

the sensors were not always placed in the center (e.g., location 4) or at all within UGS but at the edge (e.g., locations 16 and 17). Third, the disadvantages of using time series data from a citizen science monitoring project are data gaps due to e.g. sensor batteries not being replaced quickly and other data cleaning issues. Therefore, we limited the sample to 16 locations with effects on the usability and power of statistical tests. Fourth, during the observation period, 2021–2022, the La Niña Southern Oscillation (ENSO) was occurring, observed as excessive precipitation throughout large parts of our study period. It would be useful to repeat our study with data gathered during an ENSO neutral period.

Our study confirms that UGS, trees in particular, in a humid tropical climate play a key role in mitigating urban heat. Future research could focus more specifically on UGS configuration for most effective cooling in similar climate, urban development, and socio-economic contexts, taking into consideration the higher humidity of multi-layered vegetation, optimal size and patch density or shape for urban design. In this sense it is also relevant to further study which tree traits or species are most beneficial for cooling - information which is still lacking for humid tropical climates (Rahman et al., 2020). Considering quality of life and outdoor thermal comfort in the humid tropics (Antonini et al., 2020; Banerjee et al., 2020), future research can also determine which micro-climate variables are most appropriate for monitoring. Studies on the benefits of UGS cooling on indoor thermal comfort (Rodriguez and D'Alessandro, 2019) and energy consumption (Santamouris et al., 2015) are also relevant, as, unlike in temperate climates, the use of air conditioning during working hours and at night for sleeping are a more widespread practice in Paramaribo (Lachman, 2018) and other tropical cities.

5. Conclusions

Our study analyzed diurnal and seasonal patterns of twenty micro-climate variables and the effects of UGS characteristics onto the micro-climate in a humid tropical city. We drew on air temperature and humidity data collected through a citizen science-based monitoring network and satellite LST for sixteen sites in Paramaribo, Suriname. We found distinct patterns for the wet and dry seasons and confirmed that a larger share of trees in multi-layered structures is associated with stronger cooling effects in this humid tropical climate. We identified several high correlations between micro-climate variables, but also noted that variables such as average temperature and minimum nighttime temperatures measure distinct aspects of the micro-climate and may have distinct impacts on human well-being. Thus, comparing studies focusing on only one of these micro-climate variables is challenging. Our findings help address research gaps related to tropical climates and temporal scale in studies on urban climate cooling from UGS. Cooling from UGS can help cities in the humid tropics adapt to climate change. Including measurements during the wet season, something that only few studies have done so far, enables examining the influence of factors such as wetness and humidity, which play a key role in this always-hot climate. Furthermore, comparing with and learning from studies can be enhanced when a larger set of micro-climate indicators is included. This is especially relevant when developing strategies for mitigating the human health risks of increased temperatures in cities. Involving citizen scientists in such studies requires additional effort but provides multiple benefits that contribute to enriching knowledge and increasing awareness of the general public on the importance of urban vegetation for cooler surroundings in a warming world.

CRediT authorship contribution statement

Lisa Best* : Conceptualization, Methodology, Data collection, Formal Analysis, Writing – original draft, Writing – review & editing, Visualization**. Nina Schwarz* :** Conceptualization, Methodology, Data curation, Formal Analysis, Writing – original draft, Writing – review & editing, Visualization**. Davita Obergh:** Data collection, Writing – review & editing**. Adriaan J. Teuling:** Supervision, Writing – review & editing**. Rudi van Kanten:** Writing – review & editing. **Louise Willemen:** Conceptualization, Methodology, Writing – review & editing.

Declaration of Competing Interest

The authors declare that they have no known competing financial interests or personal relationships that could have appeared to influence the work reported in this paper.

Acknowledgments

We thank all citizen scientists in the umbrella project "Towards a Green and Livable Paramaribo" (groenparamaribo.org) for their contributions to prioritizing monitoring locations, collecting data and discussing data visualizations. We gratefully acknowledge funding by the UTSN Twinning facility for project number UTSN-31–123-M-G "Naar een groen en leefbaarder Paramaribo" and by the Dutch Research Council (NWO) for project number NWA.1418.20.010 ''Keeping track of changes towards healthy-living in a green urban Suriname".

Appendix

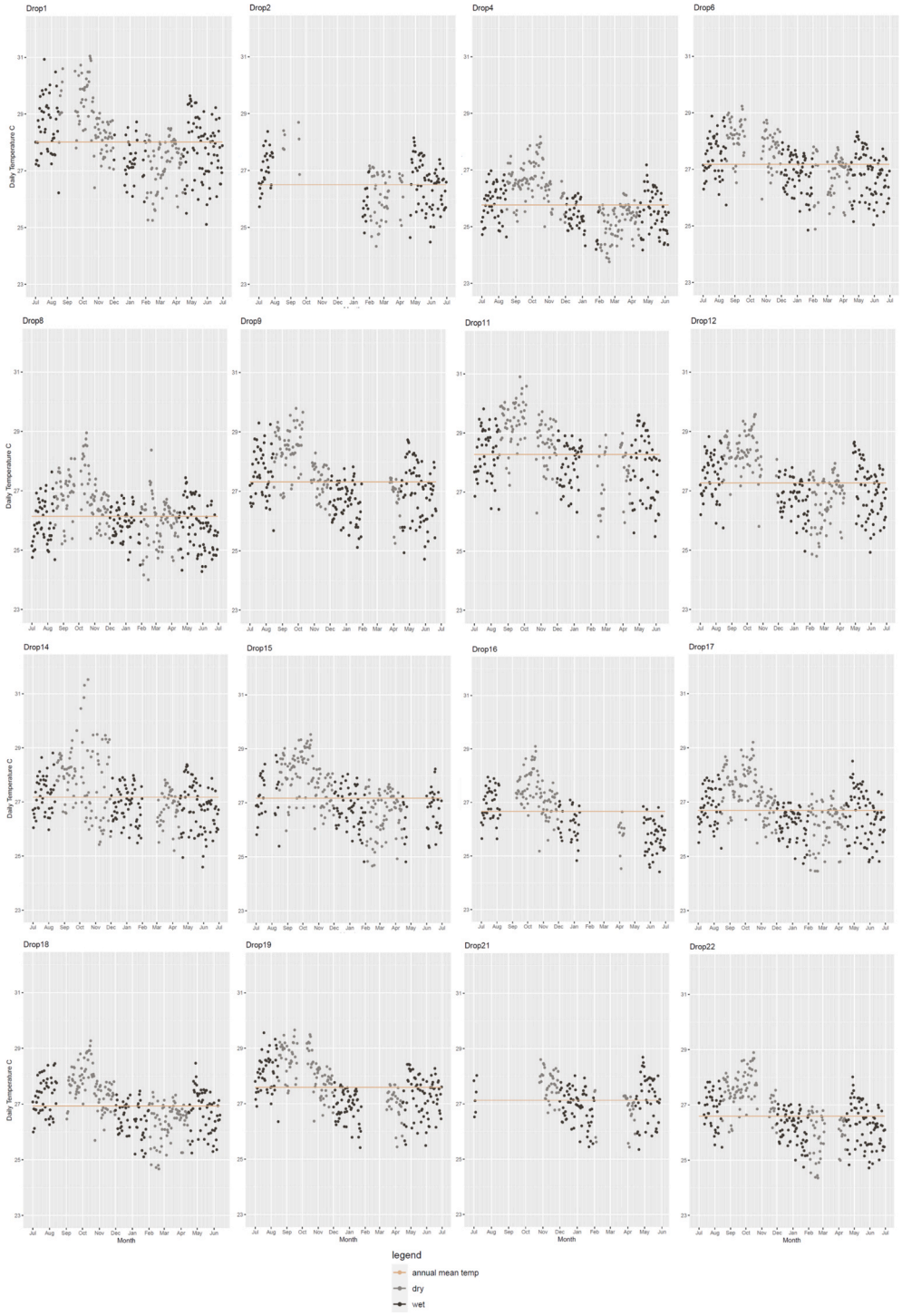

Fig. A1. a to A1k: Daily temperature means per location.

.

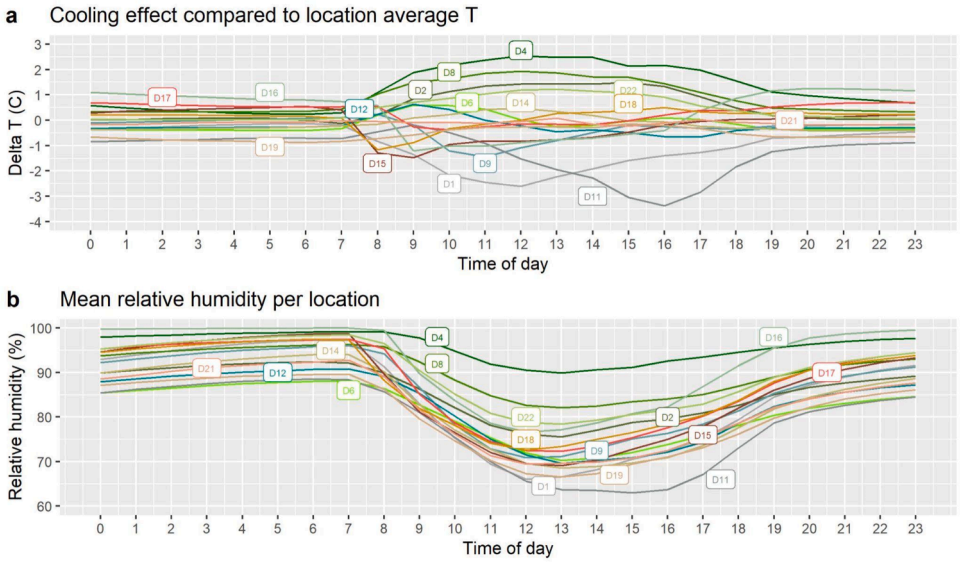

Fig. A2. Temperature (T) of measurement locations subtracted from the average of all locations (A2a), and relative humidity of each location, the numbers indicate the location IDs. The lines below zero refer to negative temperature differences ($T_{Average}$ - T_{Sensor}, Section 2.2), indicating heating, while the distance to zero indicates the extent. Locations with more and complex vegetation are depicted in dark green, larger shares of impervious surface with grey lines.

.

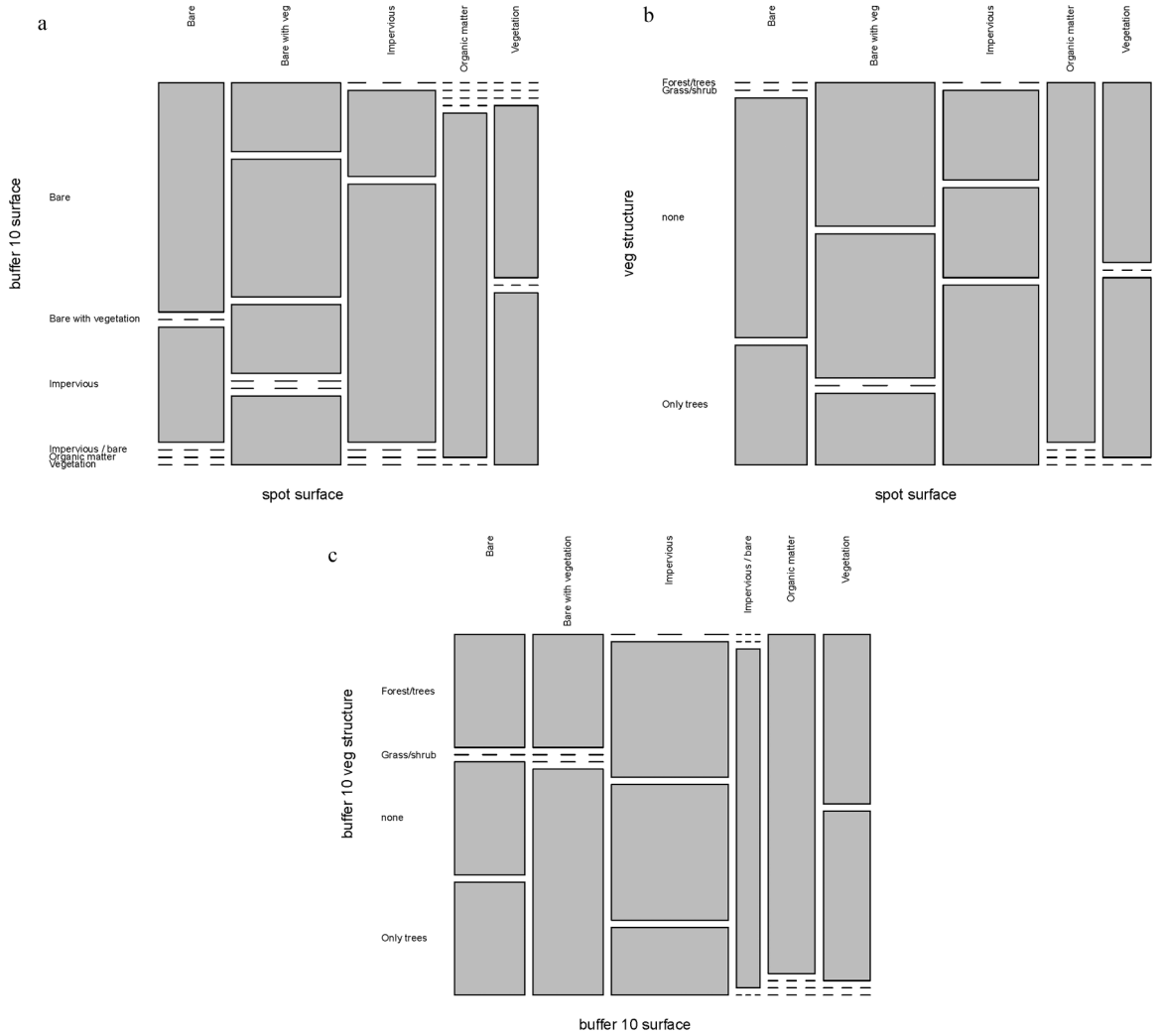

Fig. A3. a: Mosaic plots between spot surface and dominant surface in 10 m bufferb: Mosaic plots between spot surface and vegetation structure Mosaic plots between vegetation structure and dominant surface in 10 m buffer.

.

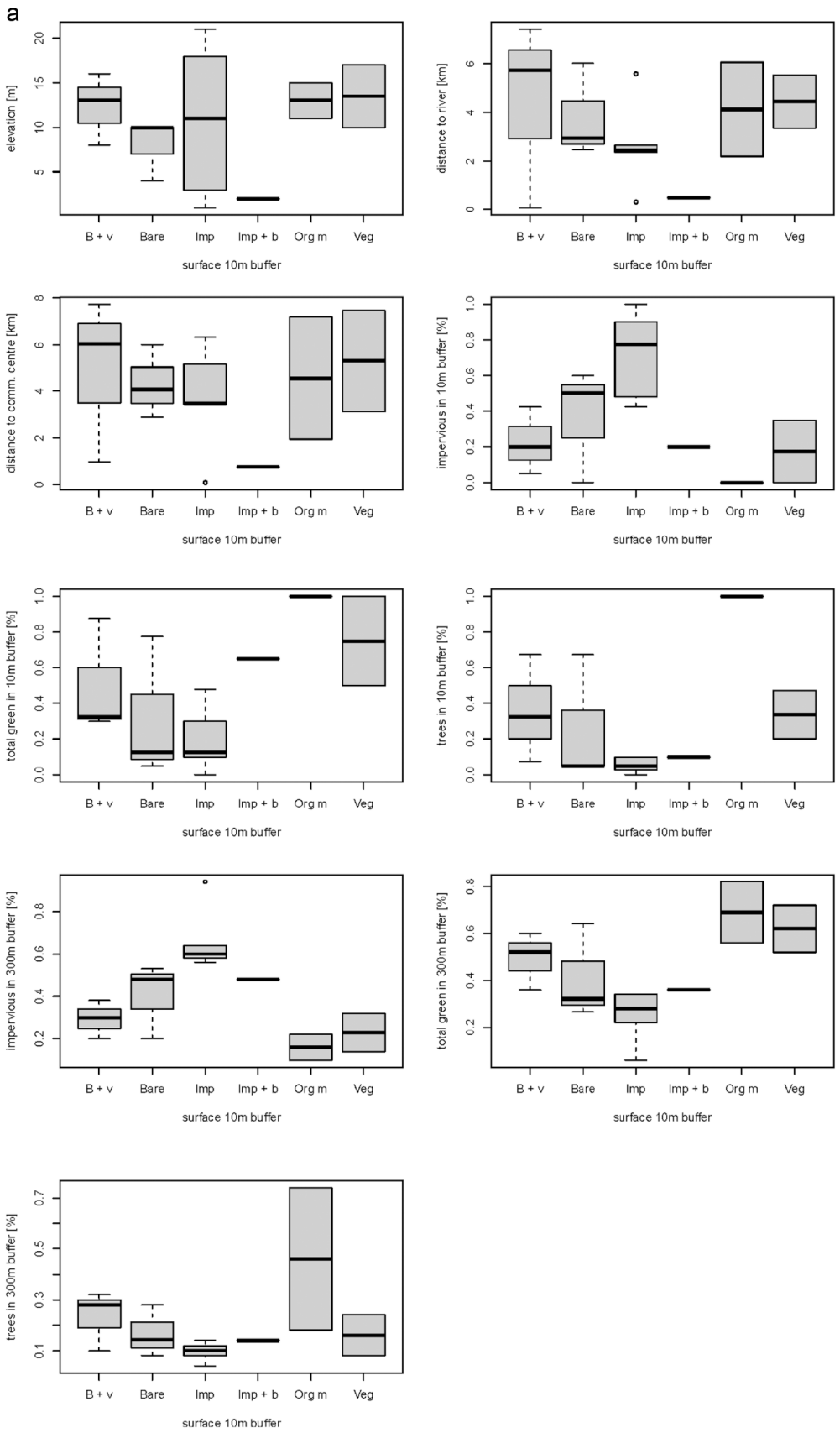

Fig. A4. a: Boxplots between surface cover in 10 m buffer and metric location characteristics. Please note: "B": Bare, "V": vegetation, "Imp": Impervious, "Org m": Organic matter b: Boxplots between vegetation structure in 10 m buffer and metric location characteristics. Please note: "F": Forest, "T": Trees c: Boxplots between surface cover under sensorand metric location characteristics. Please note: "B": Bare, "V": vegetation, "Imp": Impervious, "Org m": Organic matter.

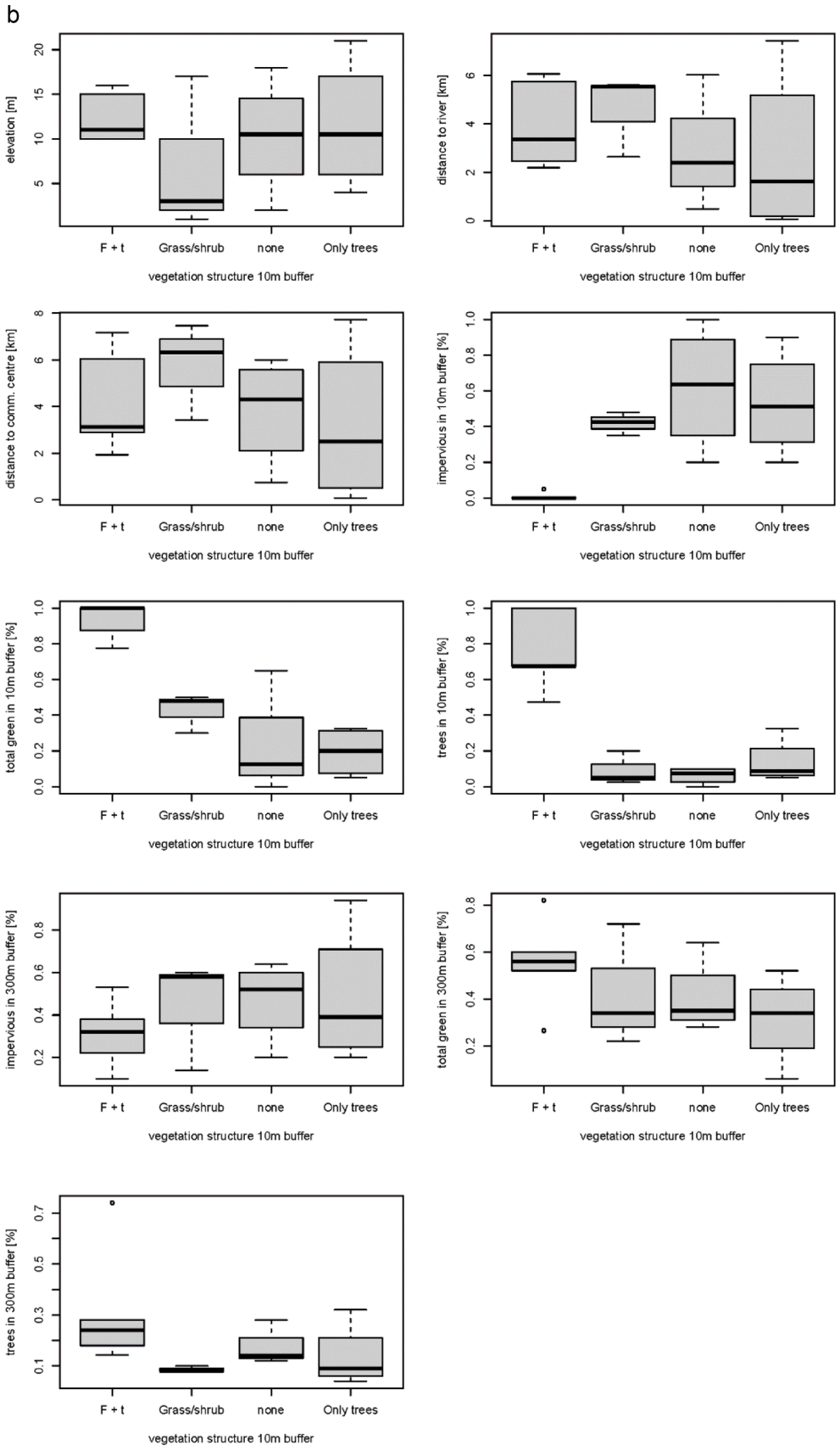

Fig. A4. (*continued*).

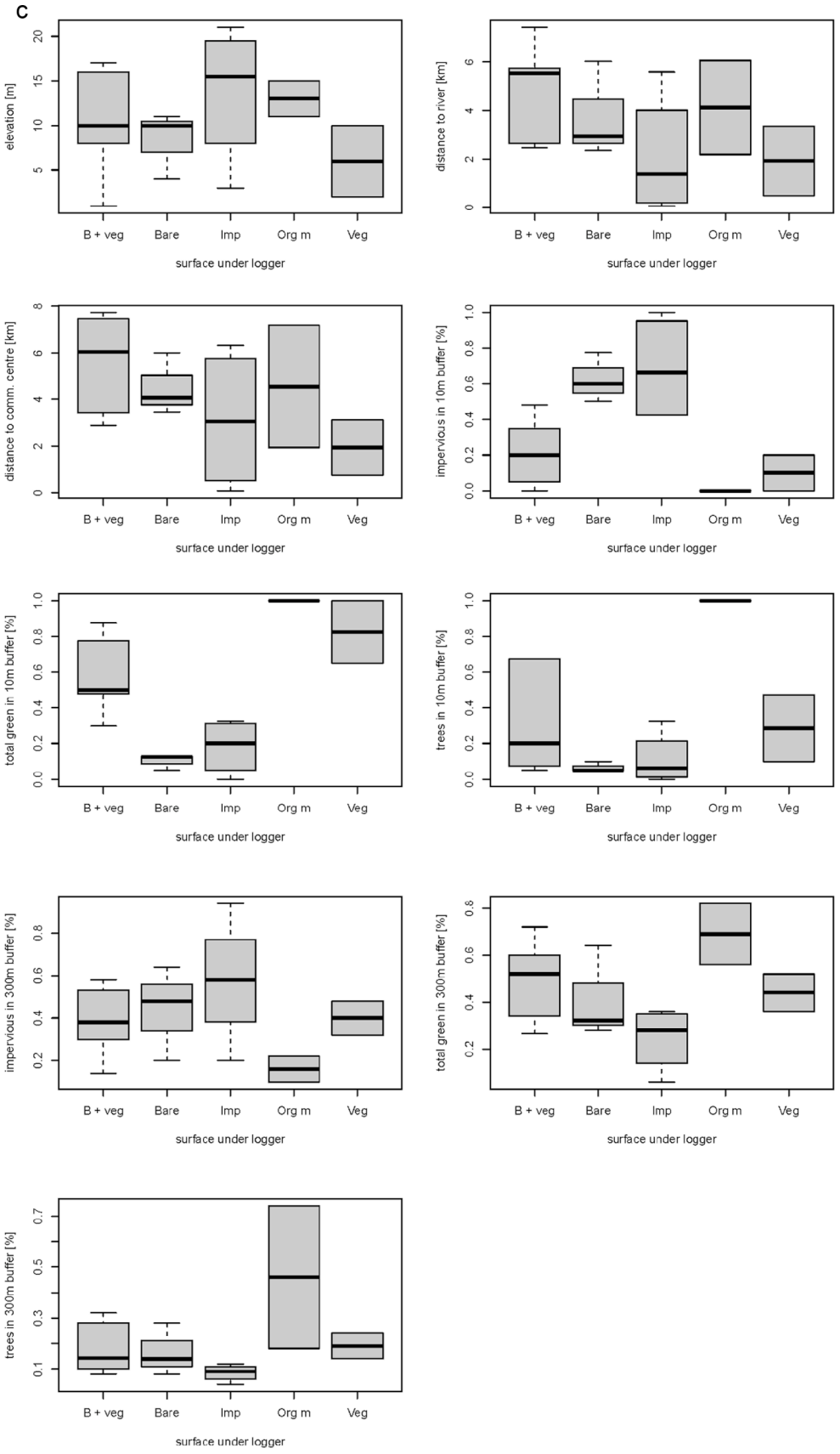

Fig. A4. (*continued*).

Table A1
Location characteristics and micro-climate variables for 16 locations.

Location / variable	1	2	4	6	8	9	11	12	14	15	16	17	18	19	21	22
Dominant surface cover 10 m buffer	Impervious	Bare	Organic matter	Bare with vegetation	Organic matter	Impervious	Impervious	Impervious / bare	Bare	Vegetation	Vegetation	Bare with vegetation	Bare	Impervious	Impervious	Bare with vegetation
Dominant vegetation structure 10 m buffer	none	Forest/trees	Forest/ trees	Only trees	Forest/ trees	Grass/shrub	Only trees	none	Only trees	Grass/shrub	Forest/ trees	Only trees	none	none	Grass/ shrub	Forest/trees
Dominant surface cover under sensor	Bare	Bare with vegetation	Organic matter	Impervious	Organic matter	Bare with vegetation	Impervious	Vegetation	Bare	Bare with vegetation	Vegetation	Bare with vegetation	Bare	Impervious	Impervious	Bare with vegetation
Elevation [m]	11	10	15	13	11	1	21	2	4	17	10	8	10	18	3	16
Distance to commercial center [km]	3.5	2.9	1.9	1.0	7.2	3.4	0.1	0.8	4.1	7.5	3.1	7.7	6.0	5.2	6.3	6.1
Distance to river [km]	2.4	2.5	2.2	0.1	6.1	2.6	0.3	0.5	2.9	5.5	3.4	7.4	6.0	2.4	5.6	5.7
Impervious in 10 m buffer [%]	0.8	0.0	0.0	0.4	0.0	0.5	0.9	0.2	0.6	0.4	0.0	0.2	0.5	1.0	0.4	0.1
Total green in 10 m buffer [%]	0.1	0.8	1.0	0.3	1.0	0.5	0.1	0.7	0.1	0.5	1.0	0.3	0.1	0.0	0.3	0.9
Trees in 10 m buffer [%]	0.1	0.7	1.0	0.3	1.0	0.1	0.1	0.1	0.1	0.2	0.5	0.1	0.1	0.0	0.0	0.7
Impervious in 300 m buffer [%]	0.6	0.5	0.1	0.2	0.2	0.6	0.9	0.5	0.5	0.1	0.3	0.3	0.2	0.6	0.6	0.4
Total green in 300 m buffer [%]	0.3	0.3	0.8	0.4	0.6	0.3	0.1	0.4	0.3	0.7	0.5	0.5	0.6	0.3	0.2	0.6
Trees in 300 m buffer [%]	0.1	0.1	0.7	0.1	0.2	0.1	0.0	0.1	0.1	0.1	0.2	0.3	0.3	0.1	0.1	0.3
Mean temperature year [°C]	28.0	26.5	25.8	27.2	26.1	27.3	28.3	27.3	27.2	27.2	26.7	26.7	26.9	27.6	27.1	26.6
Mean temperature core wet season [°C]	27.6	26.3	25.3	26.6	25.6	26.7	27.4	26.8	26.5	26.7	25.7	26.3	26.5	27.1	27.0	26.0
Mean temperature core dry season [°C]	29.3	NA	26.9	27.8	27.3	28.3	29.0	28.4	28.0	28.2	27.7	27.7	28.0	28.4	28.0	27.9
Mean humidity year [%]	84.4	85.7	95.8	81.1	90.3	85.7	78.4	82.5	82.9	86.0	92.3	87.5	87.1	80.4	82.4	90.0
Mean humidity core wet season [%]	87.4	89.9	97.7	83.7	91.9	89.5	80.0	82.4	91.2	89.6	97.3	87.8	91.2	80.0	83.1	93.7
Mean humidity core dry season [%]	81.8	NA	93.9	80.5	88.6	84.4	78.2	82.8	65.5	83.7	89.6	87.6	84.2	81.0	82.9	86.5
Minimum night-time temperature year [°C]	22.0	21.9	22.1	22.1	21.4	22.1	22.9	21.9	22.0	20.6	21.0	21.4	21.5	23.1	21.8	22.1
Minimum night-time temperature core wet season [°C]	22.2	21.9	22.3	22.1	22.1	22.3	23.5	21.9	22.3	22.0	21.8	21.9	22.8	23.1	23.3	22.2
Minimum night-time temperature core dry season [°C]	24.3	NA	24.1	24.9	23.7	24.2	25.0	24.7	25.2	23.3	23.4	23.5	23.5	25.0	24.2	24.1
Range night-time temperature year [°C]	8.6	7.1	6.0	7.6	8.1	7.7	8.0	7.9	10.8	9.0	7.0	7.5	7.3	7.5	6.7	6.9
Range night-time temperature core wet season[°C]	6.3	6.0	4.4	6.0	5.4	5.8	5.6	6.1	5.7	5.5	4.3	5.5	4.7	5.2	4.7	5.4
Range night-time temperature core dry season [°C]	6.1	NA	4.0	3.7	5.3	5.2	5.3	5.1	7.6	6.3	4.3	5.1	5.0	5.0	3.9	4.7
Maximum temperature in hot extremes [°C]	42.3	32.8	32.5	35.1	33.3	36.4	40.9	36.8	36.5	35.5	36.6	35.8	35.2	34.7	34.2	33.2
Maximum humidity in hot extremes [%]	100.0	92.3	100.0	91.4	100.0	98.6	94.5	95.6	100.0	100.0	100.0	100.0	99.8	94.2	96.1	100.0
Average standardised land surface	1.0	0.9	-0.8	-1.0	-0.7	0.9	1.7	0.8	0.3	-0.5	-0.2	-0.4	-0.9	0.7	1.1	0.5

(*continued on next page*)

Table A1 (*continued*)

Location / variable	1	2	4	6	8	9	11	12	14	15	16	17	18	19	21	22
temperature wet season [°C]																
Average standardised land surface temperature dry season [°C]	1.0	0.9	-1.0	-0.9	-0.1	0.8	1.5	-0.9	0.5	0.1	-0.4	-0.4	-1.0	0.7	0.7	0.4
Mean temperature 6:00 hrs core wet season [°C]	24.4	24.4	24.1	24.7	23.9	24.2	25.0	24.6	24.3	23.7	23.6	23.8	24.2	25.2	24.5	24.3
Mean temperature 13hrs core wet season [°C]	32.6	29.2	27.6	30.6	28.2	30.8	32.0	30.6	30.3	31.0	30.8	30.5	30.2	30.5	30.4	28.9
Mean temperature 6:00 hrs core dry season [°C]	24.8	24.6	24.4	25.1	24.3	24.6	25.4	25.0	25.3	24.1	23.8	24.1	24.4	25.6	24.7	24.7
Mean temperature 13hrs core dry season [°C]	32.8	28.7	28.3	30.9	29.0	31.9	32.9	31.3	29.9	31.4	31.8	30.7	30.2	31.1	30.3	29.7

Table A2
Landsat images used to calculate land surface temperature.

Season	Scene ID	Date and time acquired	Scene Cloud cover %
Dry season	LC82290562018312LGN00	2018–09–21 13:58:07	6.26%
Dry season	LC82290562019283LGN00	2019–10–10 13:58:34	0.40%
Dry season	LC82290562020254LGN00	2020–09–10 13:58:24	4.87%
Dry season	LC82290562021272LGN00	2021–09–29 13:58:32	9.99%
Dry season	LC92290562022267LGN00	2022–09–24 13:58:32	3.73%
Wet Season	LC82290562018216LGN00	2018–08–04 13:57:31	18.82%
Wet season	LC82290562019155LGN00	2019–06–04 13:57:56	19.24%
	2019–08–07 has slightly less cloud cover over Paramaribo, but preference given to dates further away from transition period (wet→dry and vice versa)		
Wet season	LC82290562020206LGN00	2020–07–24 13:58:06	12.01%
Wet season	LC82290562021192LGN00	2021–07–11 13:58:05	19.30%
Wet season	LC92290562022219LGN00	2022–08–07 13:58:19	10.92%

Note: Images were downloaded from Earth Explorer using the following criteria: i) Landsat 8–9 OLI/TIRS, ii) path-row 229/056; iii) search range 01/01/2018–15/10/2022, iv) land cloud cover of 0–10 (%) and 0–20% for dates in the dry and wet season respectively.

Table A3
Precipitation during 2021 and 2022 compared to a 10-year average (Meteorological Service Suriname, 2023).

Season	Short wet (Dec, Jan)	Short dry (Feb- mid Apr)	Long wet (Mid Apr- mid Aug)	Long dry (Mid Aug- Nov)
Total precipitation 2011–2021 average (mm)	347.3	262.5	1330.5	295.4
Total precipitation 2021 (mm)	453.9	225.6	1476.6	414.8
Total precipitation 2022 (mm)	601.9	316.9	1111	492

.

Table A4
Pearson correlations among location characteristics with Hommel adjustment for multiple comparisons.

	elevation	distance to river	distance to CBD	share of total green in 10 m buffer	share of trees in 10 m buffer	share of impervious in 10 m buffer	share of total green in 300 m buffer	share of trees in 300 m buffer	share of impervious in 300 m buffer
elevation	1								
distance to river	-0.09	1							
distance to CBD	-0.04	0.95 * **	1						
share of total green in 10 m buffer	-0.01	0.13	-0.01	1					
share of trees in 10 m buffer	0.28	0.09	-0.01	0.85 * *	1				
share of impervious in 10 m buffer	0.21	-0.33	-0.15	-0.9 * **	-0.74 *	1			
share of total green in 300 m buffer	0.18	0.49	0.43	0.52	0.5	-0.56	1		
share of trees in 300 m buffer	0.16	0.17	0.01	0.49	0.58	-0.5	0.71	1	
share of impervious in 300 m buffer	-0.04	-0.41	-0.37	-0.46	-0.47	0.6	-0.89 * **	-0.55	1

* $p < 0.05$, * * $p < 0.01$, * ** $p < 0.001$.

Table A5
Pearson correlations among micro-climate variables.

	Mean temperature year [C]	Mean temperature core dry season [C]	Mean temperature core wet season [C]	Mean humidity year [%]	Mean humidity core dry season [%]	Mean humidity core wet season [%]	Minimum night-time temperature year [C]	Minimum night-time temperature core dry season [C]t	Minimum night-time temperature core wet season [C]	Range night-time temperature year [C]	Range night-time temperature core dry season [C]	Range night-time temperature core wet season[C]	Maximum temperature in hot extremes [C]	Maximum humidity in hot extremes [%]	Average standardised land surface temperature wet season [C]	Average standardised land surface temperature dry season [C]
Mean temperature year [C]	1															
Mean temperature core dry season [C]	0.96 * **	1														
Mean temperature core wet season [C]	0.95 * **	0.93 * **	1													
Mean humidity year [%]	-0.84 * *	-0.73	-0.87 * *	1												
Mean humidity core dry season [%]	-0.61	-0.5	-0.58	0.73	1											
Mean humidity core wet season [%]	-0.74	-0.64	-0.82 *	0.92 * **	0.44	1										
Minimum night-time temperature year [C]	0.43	0.36	0.41	-0.51	-0.32	-0.54	1									
Minimum night-time temperature core dry season [C]	0.52	0.38	0.48	-0.68	-0.69	-0.59	0.82 *	1								
Minimum night-time temperature core wet season [C]	0.49	0.37	0.51	-0.51	-0.28	-0.54	0.6	0.41	1							
Range night-time temperature year [C]	0.43	0.39	0.37	-0.42	-0.81 *	-0.15	-0.09	0.31	-0.1	1						
Range night-time temperature core dry season [C]	0.34	0.4	0.29	-0.23	-0.65	0.01	-0.1	0.15	-0.12	0.92 * **	1					
Range night-time temperature core wet season[C]	0.47	0.59	0.51	-0.55	-0.48	-0.46	0.22	0.45	-0.25	0.51	0.46	1				
Maximum temperature in	0.82 *	0.84 *	0.7	-0.47	-0.4	-0.38	0.18	0.27	0.19	0.44	0.41	0.41	1			

(*continued on next page*)

Table A5 (*continued*)

	Mean temperature year [C]	Mean temperature core dry season [C]	Mean temperature core wet season [C]	Mean humidity year [%]	Mean humidity core dry season [%]	Mean humidity core wet season [%]	Minimum night-time temperature year [C]	Minimum night-time temperature core dry season [C]t	Minimum night-time temperature core wet season [C]	Range night-time temperature year [C]	Range night-time temperature core dry season [C]	Range night-time temperature core wet season[C]	Maximum temperature in hot extremes [C]	Maximum humidity in hot extremes [%]	Average standardised land surface temperature wet season [C]	Average standardised land surface temperature dry season [C]
hot extremes [C]																
Maximum humidity in hot extremes [%]	-0.31	-0.28	-0.38	0.65	0.28	0.67	-0.52 *	-0.66	-0.27	0.18	0.4	-0.35	0.05	1		
Average standardised land surface temperature wet season [C]	0.64	0.75	0.65	-0.56	-0.37	-0.52	0.54	0.5	0.45	0.09	0.2	0.35	0.48	-0.32	1	
Average standardised land surface temperature dry season [C]	0.57	0.68	0.57	-0.47	-0.43	-0.36	0.44	0.36	0.46	0.27	0.38	0.32	0.4	-0.18	0.82 *	1

* $p < 0.05$, * * $p < 0.01$, * ** $p < 0.001$

Table A6
Results of the Kruskal-Wallis tests for effects of vegetation structure and surface under the sensor onto micro-climate variables (upper part) and significant ($p < 0.05$) pairwise comparison (lower part of each cell).

	Vegetation structure in 10 m buffer	Surface under sensor
Mean annual temperature	$p < 0.05$ No vs Forest/trees; Only trees vs. Forest/trees at $p < 0.1$	n.s.
Mean humidity dry season	$p < 0.05$ no pairwise differences	$p < 0.05$ no pairwise differences
Mean humidity wet season	$p < 0.05$ no pairwise differences	n.s. no pairwise differences
Minimum night-time temperature dry season	n.s.	n.s.
Minimum night-time temperature wet season	n.s.	n.s.
Range night-time temperature dry season	n.s.	n.s.
Range night-time temperature wet season	n.s.	n.s.
Maximum humidity hot extremes	n.s.	n.s.
Land surface temperature dry season	n.s.	n.s.

References

Amorim, M.C., de, C.T., Dubreuil, V., Amorim, A.T., 2021. Day and night surface and atmospheric heat islands in a continental and temperate tropical environment. Urban Clim. 38. https://doi.org/10.1016/j.uclim.2021.100918.

Antonini, E., Vodola, V., Gaspari, J., de Giglio, M., 2020. Outdoor wellbeing and quality of life: a scientific literature review on thermal comfort (MDPI AG). *Energies* Vol. 13 (Issue 8). https://doi.org/10.3390/en13082079.

Aram, F., Higueras García, E., Solgi, E., Mansournia, S., García, E.H., 2019. Urban green space cooling effect in cities. Green space cooling effect in cities. Heliyon 5, 1339. https://doi.org/10.1016/j.heliyon.2019.

Arnfield, A.J., 2003. Two decades of urban climate research: a review of turbulence, exchanges of energy and water, and the urban heat island. Int. J. Climatol. 23, 1–26.

Banerjee, S., Middel, A., Chattopadhyay, S., 2020. Outdoor thermal comfort in various microentrepreneurial settings in hot humid tropical Kolkata: human biometeorological assessment of objective and subjective parameters. Sci. Total Environ. 721. https://doi.org/10.1016/j.scitotenv.2020.137741.

Bao, T., Li, X., Zhang, J., Zhang, Y., Tian, S., 2016. Assessing the distribution of urban green spaces and its anisotropic cooling distance on urban heat island pattern in Baotou, China. ISPRS Int. J. Geo-Inf. 5 (2), 12. https://doi.org/10.3390/ijgi5020012.

Binarti, F., Koerniawan, M.D., Triyadi, S., Utami, S.S., Matzarakis, A., 2020. A review of outdoor thermal comfort indices and neutral ranges for hot-humid regions. In: Urban Climate, Vol. 31. Elsevier B.V,. https://doi.org/10.1016/j.uclim.2019.100531.

Bowler, D.E., Buyung-Ali, L., Knight, T.M., Pullin, A.S., 2010. Urban greening to cool towns and cities: a systematic review of the empirical evidence. In: Landscape and Urban Planning, Vol. 97. Elsevier,, pp. 147–155. https://doi.org/10.1016/j.landurbplan.2010.05.006.

General Bureau of Statistics - Suriname (ABS), 2018. 8ste Milieustatistieken Publicatie / 8th Environment Statistics Publication. ⟨https://unstats.un.org/unsd/environment/Compendia/Suriname_Eighth%20Environment%20Statistics%20Publication%202018.pdf⟩.

Chafer, M., Tan, C.L., Cureau, R.J., Hien, W.N., Pisello, L.A., & Cabeza, L.F. , 2022. Mobile measurements of microclimatic variables through the central area of Singapore: An analysis from the pedestrian perspective. Sustainable Cities and Society, 83(May). https://doi.org/10.1016/j.scs.2022.103986.

Chow, W.T.L., Roth, M., 2006. Temporal dynamics of the urban heat island of Singapore. Int. J. Climatol. 26 (15), 2243–2260. https://doi.org/10.1002/joc.1364.

Cooper, C.B., Dickinson, J., Phillips, T., Bonney, R., 2007. Citizen science as a tool for conservation in residential ecosystems. Ecol. Soc. 12 (2). ⟨http://www.ecologyandsociety.org/vol12/iss2/art11/⟩.

Do Nascimento, A.C.L., Galvani, E., Gobo, J.P.A., Wollmann, C.A., 2022. Comparison between air temperature and land surface temperature for the city of São Paulo, Brazil. Atmosphere 13 (3). https://doi.org/10.3390/atmos13030491.

Dobbs, C., Escobedo, F.J., Clerici, N., de la Barrera, F., Eleuterio, A.A., MacGregor-Fors, I., Reyes-Paecke, S., Vásquez, A., Zea Camaño, J.D., Hernández, H.J., 2019. Urban ecosystem services in Latin America: mismatch between global concepts and regional realities. Urban Ecosyst. 22 (1), 173–187. https://doi.org/10.1007/s11252-018-0805-3.

Du, C., Jia, W., Chen, M., Yan, L., Wang, K., 2022. How can urban parks be planned to maximize cooling effect in hot extremes? Linking maximum and accumulative perspectives. J. Environ. Manag. 317. https://doi.org/10.1016/j.jenvman.2022.115346.

Ebi, K.L., Capon, A., Berry, P., Broderick, C., de Dear, R., Havenith, G., Honda, Y., Kovats, R.S., Ma, W., Malik, A., Morris, N.B., Nybo, L., Seneviratne, S.I., Vanos, J., Jay, O., 2021. Hot weather and heat extremes: health risks. The Lancet 398 (10301), 698–708. https://doi.org/10.1016/S0140-6736(21)01208-3.

Feyisa, G.L., Dons, K., Meilby, H., 2014. Efficiency of parks in mitigating urban heat island effect: an example from Addis Ababa. Landsc. Urban Plan. 123, 87–95. https://doi.org/10.1016/j.landurbplan.2013.12.008.

Fu, J., Dupre, K., Tavares, S., King, D., 2022. Optimized greenery configuration to mitigate urban heat: a decade systematic review. Front. Archit. Res. 11 (3), 466–491. https://doi.org/10.1016/j.foar.2021.12.005.

Fung-Loy, K., Van Rompaey, A., Hemerijckx, L.M., 2019. Detection and simulation of urban expansion and socioeconomic segregation in the greater Paramaribo Region, Suriname. Tijdschr. Voor Econ. En. Soc. Geogr. 0 (0), 1–20. https://doi.org/10.1111/tesg.12350.

General Bureau of Statistics - Suriname (ABS). 2021. Statistisch Jaarboek 2019/2020 Suriname / Statistical Yearbook 2019/2020 Suriname. https://statistics-suriname.org/wp-content/uploads/2021/08/Statistisch-Jaarboek_Statistical-Yearbook-2019-2020.pdf.

Giridharan, R., Emmanuel, R., 2018. The impact of urban compactness, comfort strategies and energy consumption on tropical urban heat island intensity: a review. Sustain. Cities Soc. 40, 677–687. https://doi.org/10.1016/j.scs.2018.01.024.

Hamada, S., Ohta, T., 2010. Seasonal variations in the cooling effect of urban green areas on surrounding urban areas. Urban For. Urban Green. 9, 15–24. https://doi.org/10.1016/j.ufug.2009.10.002.

Hubbart, J.A., 2011. An inexpensive alternative solar radiation shield for ambient air temperature micro-sensors. J. Nat. Environ. Sci. 2 (2), 9–14.

IPCC, 2021. Climate change 2021: The physical science basis. Contribution of Working Group I to the Sixth Assessment Report of the Intergovernmental Panel on Climate Change. https://doi.org/10.1017/9781009157896.

Jaganmohan, M., Knapp, S., Buchmann, C.M., Schwarz, N., 2016. The bigger, the better? The influence of urban green space design on cooling effects for residential areas. J. Environ. Qual. 45 (1), 134–145. https://doi.org/10.2134/jeq2015.01.0062.

Keeler, B.L., Hamel, P., McPhearson, T., Hamann, M.H., Donahue, M.L., Meza Prado, K.A., Arkema, K.K., Bratman, G.N., Brauman, K.A., Finlay, J.C., Guerry, A.D., Hobbie, S.E., Johnson, J.A., MacDonald, G.K., McDonald, R.I., Neverisky, N., Wood, S.A., 2019. Social-ecological and technological factors moderate the value of urban nature. Nat. Sustain. 2 (1), 29–38. https://doi.org/10.1038/s41893-018-0202-1.

Klemann-Junior, L., Vallejos, M.A.V., Scherer-Neto, P., Vitule, J.R.S., 2017. Traditional scientific data Vs. Uncoordinated citizen science effort: a review of the current status and comparison of data on avifauna in Southern Brazil. PLOS One 12 (12). https://doi.org/10.1371/journal.pone.0188819.

Lachman, D.A., 2018. Re-energizing suriname with less energy. J. Environ. Sci. Public Health 02 (02). https://doi.org/10.26502/jesph.96120032.

Li, H., Meng, H., He, R., Lei, Y., Guo, Y., Ernest, A., atta, Jombach, S., Tian, G., 2020. Analysis of cooling and humidification effects of different coverage types in small green spaces (SGS) in the context of urban homogenization: a case of HAU campus green spaces in summer in Zhengzhou, China. Atmosphere 11 (8). https://doi.org/10.3390/ATMOS11080862.

Liu, H., Huang, B., Zhan, Q., Gao, S., Li, R., Fan, Z., 2021. The influence of urban form on surface urban heat island and its planning implications: evidence from 1288 urban clusters in China. Sustain. Cities Soc. 71. https://doi.org/10.1016/j.scs.2021.102987.

Maclean, I.M.D., Duffy, J.P., Haesen, S., Govaert, S., De Frenne, P., Vanneste, T., Lenoir, J., Lembrechts, J.J., Rhodes, M.W., Van Meerbeek, K., 2021. On the measurement of microclimate. Methods Ecol. Evol. 12 (8), 1397–1410. https://doi.org/10.1111/2041-210X.13627.

Masoudi, M., Tan, P.Y., Liew, S.C., 2019. Multi-city comparison of the relationships between spatial pattern and cooling effect of urban green spaces in four major Asian cities. Ecol. Indic. 98, 200–213. https://doi.org/10.1016/j.ecolind.2018.09.058.

Meteorological Service Suriname, 2023. Precipitation data for Suriname. ⟨https://dondru.sr/⟩.

Naserikia, M., Hart, M.A., Nazarian, N., Bechtel, B., 2022. Background climate modulates the impact of land cover on urban surface temperature. Sci. Rep. 12 (1) https://doi.org/10.1038/s41598-022-19431-x.

Obradovich, N., Migliorini, R., Mednick, S.C., Fowler, J.H., 2017. Nighttime temperature and human sleep loss in a changing climate. Sci. Adv. 3 (e160155). ⟨https://www.science.org⟩.

Park, J., Kim, J.H., Lee, D.K., Park, C.Y., Jeong, S.G., 2017. The influence of small green space type and structure at the street level on urban heat island mitigation. Urban For. Urban Green. 21, 203–212. https://doi.org/10.1016/j.ufug.2016.12.005.

Priya, U.K., Senthil, R., 2021. A review of the impact of the green landscape interventions on the urban microclimate of tropical areas. Build. Environ. 205. https://doi.org/10.1016/j.buildenv.2021.108190.

Rahman, M.A., Stratopoulos, L.M.F., Moser-Reischl, A., Zölch, T., Häberle, K.H., Rötzer, T., Pretzsch, H., Pauleit, S., 2020. Traits of trees for cooling urban heat islands: a meta-analysis. Build. Environ. 170. https://doi.org/10.1016/j.buildenv.2019.106606.

Remijn, T., Best, L., van Kanten, R., Schwarz, N., & Willemen, L. 2020. Dry season standardised maximum land surface temperature of the Greater Paramaribo Region 2015–2019, product of 'Naar een groen en leefbaarder Paramaribo' by Tropenbos Suriname and University of Twente-ITC. https://doi.org/10.5281/zenodo.7696767.

Ren, Z., Fu, Y., Dong, Y., Zhang, P., He, X., 2022. Rapid urbanization and climate change significantly contribute to worsening urban human thermal comfort: a national 183-city, 26-year study in China. Urban Clim. 43. https://doi.org/10.1016/j.uclim.2022.101154.

Richards, D.R., Fung, T.K., Belcher, R.N., Edwards, P.J., 2020. Differential air temperature cooling performance of urban vegetation types in the tropics. Urban For. Urban Green. 50. https://doi.org/10.1016/j.ufug.2020.126651.

Rodriguez, C.M., D'Alessandro, M., 2019. Indoor thermal comfort in the tropics. Int. Assoc. Urban Clim. 73, 9–15. ⟨https://re.public.polimi.it/retrieve/handle/11311/1141262/525346/Urban%20Climat%20News_Indoor%20thermal%20comfort%20in%20the%20tropics.pdf⟩.

Roth, M., 2007. Review of urban climate research in (sub)tropical regions. Int. J. Climatol. 27 (14), 1859–1873. https://doi.org/10.1002/joc.1591.

Santamouris, M., Cartalis, C., Synnefa, A., Kolokotsa, D., 2015. On the impact of urban heat island and global warming on the power demand and electricity consumption of buildings - a review. Energy Build. 98, 119–124. https://doi.org/10.1016/j.enbuild.2014.09.052.

Sayer, J., Margules, C., Bohnet, I., Boedhihartono, A., Pierce, R., Dale, A., Andrews, K., 2015. The role of citizen science in landscape and seascape approaches to integrating conservation and development. Land 4 (4), 1200–1212. https://doi.org/10.3390/land4041200.

Schwarz, N., Schlink, U., Franck, U., Großmann, K., 2012. Relationship of land surface and air temperatures and its implications for quantifying urban heat island indicators - an application for the city of Leipzig (Germany). Ecol. Indic. 18, 693–704. https://doi.org/10.1016/j.ecolind.2012.01.001.

State of the Tropics, 2014. State of the Tropics 2014 Report. ⟨https://www.jcu.edu.au/state-of-the-tropics/publications/2014-state-of-the-tropics-report⟩.

State of the Tropics, (2020). State of the Tropics 2020 Report. ⟨https://www.jcu.edu.au/state-of-the-tropics/publications/state-of-the-tropics-2020-report⟩.

Taus, R., Best, L., van Kanten, R., Schwarz, N., & Willemen, L. (2019). Land cover map of the Greater Paramaribo Region 2019. In Product of "Naar een groen en leefbaarder Paramaribo" by Tropenbos Suriname and University of Twente-ITC. https://doi.org/10.5281/zenodo.7696951.

Vickerstaff, V., Omar, R.Z., Ambler, G., 2019. Methods to adjust for multiple comparisons in the analysis and sample size calculation of randomised controlled trials with

multiple primary outcomes. BMC Med. Res. Methodol. 19 (1) https://doi.org/10.1186/s12874-019-0754-4.

Wang, C., Ren, Z., Dong, Y., Zhang, P., Guo, Y., Wang, W., Bao, G., 2022. Efficient cooling of cities at global scale using urban green space to mitigate urban heat island effects in different climatic regions. Urban For. Urban Green. *74*. https://doi.org/10.1016/j.ufug.2022.127635.

Wang, Z., Li, Y., Song, J., Wang, K., Xie, J., Wai, P., Ren, C., Di, S., 2022. Urban climate modelling and optimizing tree planning for urban climate in a subtropical high-density city. Urban Clim. 43 (February), 101141 https://doi.org/10.1016/j.uclim.2022.101141.

Wehn, U., Gharesifard, M., Ceccaroni, L., Joyce, H., Ajates, R., Woods, S., Bilbao, A., Parkinson, S., Gold, M., Wheatland, J., 2021. Impact assessment of citizen science: state of the art and guiding principles for a consolidated approach. In: Sustainability Science, 16. Springer,, Japan, pp. 1683–1699. https://doi.org/10.1007/s11625-021-00959-2.

Weidum, C. , 2014. Urban Sprawl in Paramaribo: the neglected opportunity to sustain communities in the fringe [Anton de Kom University of Suriname]. ⟨https://vdocuments.mx/urban-sprawl-in-paramaribo-people-want-neighbourhoods-with-safe-streets-and-good.html?page=2⟩.

World Meteorological Organization (WMO, 2021. Guide to instruments and methods of observation (WMO-No. 8). Volume III. ⟨https://library.wmo.int/doc_num.php?explnum_id=11613⟩.

Yan, H., Fan, S., Guo, C., Hu, J., Dong, L., 2014. Quantifying the impact of land cover composition on intra-urban air temperature variations at a mid-latitude city. PLOS One 9 (7). https://doi.org/10.1371/journal.pone.0102124.